

Synthesis, Characterization, Catalytic and Antiamoebic Activity of Vanadium Complexes of Binucleating Bis(dibasic tridentate ONS donor) Ligand Systems

Mannar R. Maurya,^{*[a]} Chanchal Haldar,^[a] Aftab Alam Khan,^[a] Amir Azam,^[b]
Attar Salahuddin,^[b] Amit Kumar,^[c] and Joao Costa Pessoa^{*[c]}

Keywords: Vanadium / Enzyme models / Antiprotozoal agents / Hydrazones / EPR spectroscopy / NMR spectroscopy

[V^{IV}O(acac)₂] (acac = acetylacetonate) was treated with ligands CH₂(H₂L)₂ in methanol heated at reflux to yield two neutral binuclear V^{IV} complexes with the formula [CH₂{V^{IV}OL(H₂O)}₂], namely, **1** and **2**. Ligands CH₂(H₂L)₂ **I** and **II** were derived from 5,5'-methylenebis(salicylaldehyde) and *S*-benzylthiocarbamate [CH₂(H₂sal-sbdt)₂, **I**] or *S*-methylthiocarbamate [CH₂(H₂sal-smtdt)₂, **II**]. Aerial oxidation of **1** and **2** in the presence of KOH or CsOH·H₂O resulted in the formation of dioxidovanadium(V) complexes, K₂[CH₂{V^{VO}2(sal-sbdt)}₂]·2H₂O (**3**), Cs₂[CH₂{V^{VO}2(sal-sbdt)}₂]·2H₂O (**4**), K₂[CH₂{V^{VO}2(sal-smtdt)}₂]·2H₂O (**5**) and Cs₂[CH₂{V^{VO}2(sal-smtdt)}₂]·2H₂O (**6**). The compounds were characterized in the solid state and in solution, namely, by spectroscopic techniques (IR, UV/Vis, EPR, ¹H, ¹³C and ⁵¹V NMR spectroscopy). It is demonstrated that the V^{VO}2 complexes **3–6** are efficient and selective towards the oxidative bromination by H₂O₂ of styrene to yield 1,2-dibromo-1-phenyl-

ethane, 1-phenylethane-1,2-diol and 2-bromo-1-phenylethane-1-ol, and of salicylaldehyde to yield 5-bromosalicylaldehyde, 3,5-dibromosalicylaldehyde and 2,4,6-tribromophenol; they therefore act as functional models of vanadium-dependent haloperoxidases. It is also shown that Cs₂[CH₂{V^{VO}2(sal-sbdt)}₂]·2H₂O (**4**) and Cs₂[CH₂{V^{VO}2(sal-smtdt)}₂]·2H₂O (**6**) are catalyst precursors for the catalytic oxidation of styrene by peroxide to yield styrene oxide, benzaldehyde, 1-phenylethane-1,2-diol, benzoic acid and phenylacetaldehyde. Plausible intermediates involved in these catalytic processes were established by UV/Vis, EPR and ⁵¹V NMR spectroscopic studies. The V^{VO}2 complexes along with ligands **I** and **II** were also screened against HM1:1MSS strains of *Entamoeba histolytica*; the IC₅₀ values of compounds **3**, **4** and **5** were significantly lower than that of metronidazole, thereby suggesting that they may be promising drugs for the treatment of amoebiasis.

Introduction

Interest in the coordination chemistry of vanadium, with particular emphasis on its biological,^[1–3] structural^[2,4] and catalytic properties^[5–8] has increased over the past two decades. Vanadate-dependent haloperoxidase enzymes (VHPO)^[9] and the covalent bonding of the imidazole moiety of a histidine residue through N^ε to vanadate in the active site have stimulated the design of structural models.^[10] These structural models have been extended to functional similarities in that vanadium complexes also model the oxidative halogenation and sulfoxidation of organic

substrates.^[5–8] Homogeneous vanadium (IV and V) complexes as well as their immobilized analogues also catalyze other organic reactions such as the epoxidation of alkenes,^[11–14] the hydroxylation of hydrocarbons,^[15] hydro- and oxidative amination^[16] and the oxidation of alcohols to aldehydes and ketones,^[17,18] thus showing their influence on the yield and selectivity in chemical transformations.

Prospective therapeutic applications of vanadium compounds, particularly in the treatment of *Diabetes mellitus* and cancer, and more recently in vitro antiamoebic activity against *Entamoeba histolytica* and antitrypanosomal activity against *Trypanosoma cruzi*, have also stimulated further developments in the coordination chemistry of vanadium.^[3,19] Among all parasites, the intestinal parasite *Entamoeba histolytica*, which affects millions of people worldwide and especially those in tropical developing countries, is responsible for amoebic colitis and amoebic liver abscesses. The World Health Organization in its most recent estimates has placed the death toll from amoebiasis at 40000–100000 lives annually. Approximately 90% of patients with mild to moderate amoebic dysentery respond to metronidazole (MNZ), an important drug that is applied in treatments.^[20–22] However, this drug causes several side

[a] Department of Chemistry, Indian Institute of Technology Roorkee, Roorkee 247667, India
Fax: +91-1332-273560
E-mail: rkmanfcy@iitr.ernet.in

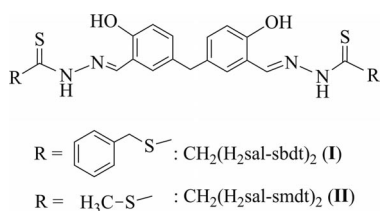
[b] Department of Chemistry, Jamia Millia Islamia, Jamia Nagar, New Delhi 100025, India

[c] Centro de Química Estrutural, Instituto Superior Técnico, Technical University of Lisbon, Av Rovisco Pais, 1049-001 Lisboa, Portugal
Fax: +351-21-8464455
E-mail: joao.pessoa@ist.utl.pt

Supporting information for this article is available on the WWW under <http://dx.doi.org/10.1002/ejic.201200012>.

effects in patients. MNZ also induces certain tumours in rodents and is mutagenic towards bacteria.^[23–27] Therefore, research on the new drugs for the treatment is a relevant therapeutic demand.

Dioxidovanadium(V) complexes of ONO, ONN and ONS donor ligands have shown very convincing results on the in vitro activity against *Entamoeba histolytica*.^[28,29] We recently described binuclear V^{IV}O and V^{VO}₂ complexes of binucleating bis(dibasic tridentate ONO donor) ligands and have studied their reactivity and catalytic and antiamoebic activity.^[29] Their good reactivity patterns and catalytic and antiamoebic activity encouraged us to consider binucleating bis(dibasic tridentate ONS donor) ligands, and we now describe the synthesis and characterization of binuclear V^{IV}O and V^{VO}₂ complexes of ligands **I** and **II** derived from 5,5'-methylenebis(salicylaldehyde) [CH₂(Hsal)₂] and *S*-benzylthiocarbamate (sbdt) or *S*-methylthiocarbamate (smdt; Scheme 1).

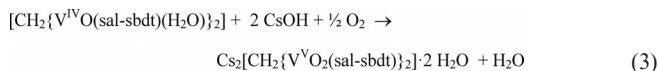
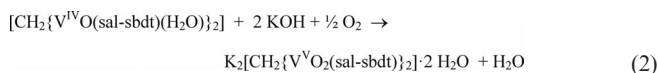
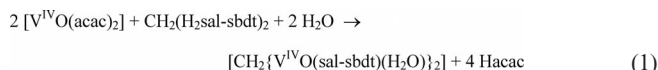


Scheme 1. Structure of the ligands designated by **I** and **II** used in this work.

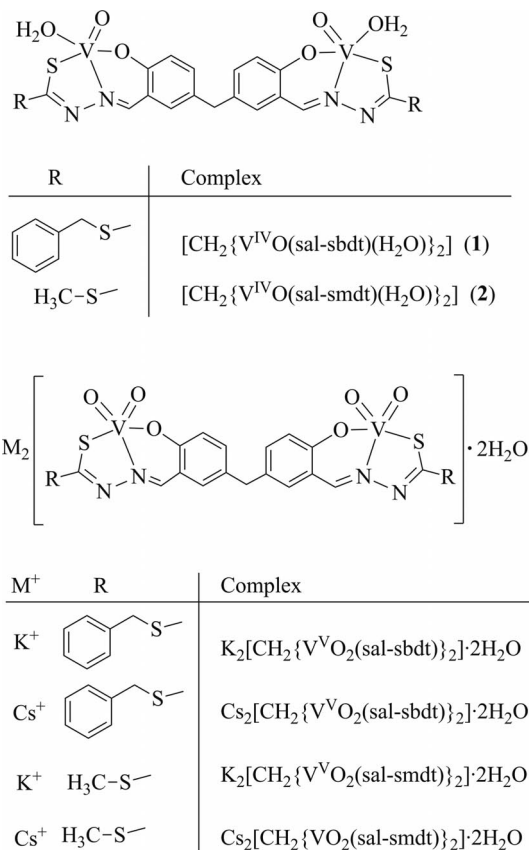
The haloperoxidase activity was confirmed by studying the oxidative bromination of salicylaldehyde and styrene when using the V^{VO}₂ complexes as catalyst precursors. In addition, the activity for catalytic oxidations was demonstrated through the oxidation of styrene by peroxide. The V^{VO}₂ complexes have also been screened against HM1:1MSS strains of *Entamoeba histolytica*.

Results and Discussion

[V^{IV}O(acac)₂] (acac = acetylacetonate) was treated with the binucleating ligands CH₂(H₂sal-sbdt)₂ (**I**) or CH₂(H₂sal-smdt)₂ (**II**) in a 2:1 molar ratio in methanol heated at reflux to give the binuclear oxidovanadium(IV) complexes [CH₂{V^{IV}O(sal-sbdt)(H₂O)}₂] (**1**) and [CH₂{V^{IV}O(sal-smdt)(H₂O)}₂] (**2**), respectively. Oxidation of **1** and **2** in the presence of KOH or CsOH·H₂O gave the corresponding V^{VO}₂ species K₂[CH₂{V^{VO}₂(sal-sbdt)₂}·2H₂O (**3**), Cs₂[CH₂{V^{VO}₂(sal-sbdt)₂}·2H₂O (**4**), Cs₂[CH₂{V^{VO}₂(sal-smdt)₂}·2H₂O (**5**) and Cs₂[CH₂{V^{VO}₂(sal-smdt)₂}·2H₂O (**6**). These complexes were also isolated directly by the reaction of [V^{IV}O(acac)₂] with **I** or **II** in a 2:1 ratio in methanol heated at reflux followed by aerial oxidation in the presence of the corresponding hydroxides. Here the reaction probably proceeds through the formation of the V^{IV}O complexes **1** and **2**. Equations (1), (2) and (3) summarize the synthetic procedures by using CH₂(H₂sal-sbdt)₂ as a representative ligand.



All complexes are soluble in methanol, DMSO and DMF. Complexes **1** and **2** exhibit magnetic moment values of 1.73 and 1.71 μ_B, respectively, which is within the expected range reported for magnetically dilute d¹ systems. Proposed structures of these complexes (Scheme 2) are based on their spectroscopic characterization (IR; electronic; EPR; ¹H and ⁵¹V NMR spectroscopy) and elemental analyses. The ligands coordinate through each of their dianionic (ONS)²⁻ thioenolate tautomeric forms.



Scheme 2. Schematic structural formulae of the V^{IV}O and V^{VO}₂ complexes that were prepared.

IR Spectral Studies

The IR spectra of a representative ligand and of the corresponding VVO_2 complex are presented in Figure S1 in the Supporting Information, and a partial list of IR spectroscopic data for ligands and complexes is presented in Table 1. The ligands exhibit a sharp band at 1030 (**I**) and 1039 cm^{-1} (**II**) due to $\nu(C=S)$ and a broad weak band in the region 3090 to 3250 cm^{-1} due to $\nu(NH)$. The disappearance of these bands in the spectra of complexes indicates the thioenolization of the $>C=S$ group and coordination of sulfur to vanadium. The presence of medium-intensity bands at 325 (**1**) and 330 (**2**) cm^{-1} due to $\nu(V-S)$ gives further evidence for the coordination of sulfur to vanadium in these complexes in the solid state. The $\nu(C=N_{\text{azomethine}})$ bands of the ligands appear at 1625 (in **I**) and 1624 cm^{-1} (in **II**). These bands show up at 1609–1613 cm^{-1} in complexes **1–6**, thereby suggesting the coordination of the azomethine nitrogen atom. Bands that appear at 948 (in **I**) and 936 cm^{-1} (in **II**) are assigned to the $\nu(N-N)$ stretch. Upon complex formation, a shift to higher frequency of the $\nu(N-N)$ band is expected because of the diminished repulsion between the lone pairs of adjacent nitrogen atoms,^[30] and we assign this band to a peak that appears in the range 1027–1034 cm^{-1} (Table 1). The $V^{IV}O$ complexes exhibit bands at 994 (**1**) and 996 cm^{-1} (**2**) due to the $\nu(V=O)$ stretch. The VVO_2 complexes exhibit one sharp band in the 884–887 cm^{-1} region and a weaker one at approximately 928–939 cm^{-1} due to $\nu_{\text{sym}}(O=V=O)$ and $\nu_{\text{asym}}(O=V=O)$. These bands confirm the *cis*- VVO_2 structure in the complexes.^[4] The weakening of one of the bands may be considered to suggest that the O atoms of the VVO_2 units are

Table 1. IR data of the compounds prepared ($\tilde{\nu}$ in cm^{-1}) and the corresponding assignments.

Compounds	$\nu(C=S)$	$\nu(C=N)$	$\nu(V=O)$	$\nu(N-N)$
$CH_2(H_2sal-sbdt)_2$ (I)	1030	1625		948
$CH_2(H_2sal-smdt)_2$ (II)	1039	1624		936
$[CH_2\{V^{IV}O(sal-sbdt)(H_2O)\}_2]$ (1)		1609	994	1034
$K_2[CH_2\{V^{VO}_2(sal-sbdt)\}_2] \cdot 2H_2O$ (3)		1613	884, 935	1027
$CS_2[CH_2\{V^{VO}_2(sal-sbdt)\}_2] \cdot 2H_2O$ (4)		1612	887, 928	1027
$[CH_2\{V^{IV}O(sal-smdt)(H_2O)\}_2]$ (2)		1609	996	1034
$K_2[CH_2\{V^{VO}_2(sal-smdt)\}_2] \cdot 2H_2O$ (5)		1612	886, 939	1030
$CS_2[CH_2\{V^{VO}_2(sal-smdt)\}_2] \cdot 2H_2O$ (6)		1612	887, 927	1033

Table 2. 1H NMR spectroscopic data (δ in ppm) of ligands and complexes recorded in $[D_6]DMSO$.

Compd. ^[a,b]	$-CH=N-$	Aromatic H	$-CH_2-$	$-OH$	$-NH$	$-SCH_2-$	$-CH_3$
I	8.50(s, 2 H)	6.80 (d, 2 H), 7.50 (d, 2 H), 7.35 (m, 12 H)	3.75 (s, 2 H)	13.35 (s, 2 H)	10.10 (s, 2 H)	4.50 (s, 4 H)	
3	9.02(s, 2 H)	6.78(d, 2 H), 7.0–7.80(m, 14 H)	3.89(s, 2 H)			4.39(s, 4 H)	
($\Delta\delta$)	(0.52)		(0.14)			(–0.11)	
4	9.03 (s, 2 H)	6.77 (d, 2 H), 7.35–7.75 (m, 14 H)	3.89 (s, 2 H)			4.39 (s, 4 H)	
($\Delta\delta$)	(0.53)		(0.14)			(–0.11)	
II	8.45 (s, 2 H)	6.8 (d, 2 H), 7.4 (d, 2 H), 7.55 (d, 2 H)	3.80 (s, 2 H)	13.32 (s, 2 H)	10.11 (s, 2 H)		2.5 (s, 6 H)
5	8.96 (s, 2 H)	6.77 (d, 2 H), 7.26 (d, 2 H), 7.51 (d, 2 H)	3.87 (s, 2 H)				2.50 (s, 6 H)
($\Delta\delta$)	(0.51)		(0.07)				(0.03)
6	8.96 (s, 2 H)	6.7 (d, 2 H), 7.26 (d, 2 H), 7.50 (d, 2 H)	3.86 (s, 2 H)				2.50 (s, 6 H)
($\Delta\delta$)	(0.52)		(0.08)				(0.03)

[a] Letters given in parentheses indicate the signal structure: s = singlet, br. = broad (unresolved), m = multiplet. [b] $\Delta\delta = \delta(\text{complex}) - \delta(\text{ligand})$.

probably involved in binding to K^+/Cs^+ in the crystal structure; such binding was confirmed in anionic dioxidovanadium(V) complexes.^[31,32]

Electronic Spectral Studies

Ligands **I** and **II** exhibit absorption bands at around 206, 255, 328 and 360 nm, which are assigned to $\phi \rightarrow \phi^*$, $\pi \rightarrow \pi_1^*$, $\pi \rightarrow \pi_2^*$, and $n \rightarrow \pi^*$ transitions, respectively. Similar slightly shifted bands are also observed in the corresponding complexes (Table S1 in the Supporting Information). In addition, a new band of medium intensity appears at approximately 405 nm, which is assigned to a ligand-to-metal charge transfer (LMCT) band.

Upon dissolution, the $V^{IV}O$ complexes have a tendency to hydrolyze and oxidize (see below). Three bands at 575, 680 and 845 nm (in **1**) and at 565, 675 and 875 nm (in **2**), observed at higher concentration, are assigned to d–d transitions. However, it is probable that these bands might be due to the presence of more than one type of $V^{IV}O$ complex in solution. For the VVO_2 complexes no such bands were detected.

1H NMR Spectroscopic Studies

Table 2 summarizes data of the 1H NMR spectra of the ligands and VVO_2 complexes, whereas Figure S2 in the Supporting Information presents the representative 1H NMR spectra of **II** and of complex **6**. The 1H NMR spectra of ligands exhibit singlets at $\delta = 13.35$ ppm (**I**) and at $\delta = 13.32$ ppm (**II**) due to phenolic protons. The absence of this signal in the complexes indicates the coordination of the phenolate oxygen atoms. Similarly, the disappearance of the signals that appear at $\delta = 10.10$ ppm (**I**) and $\delta = 10.11$ ppm (**II**) due to $-NH$ protons is in agreement with the thioenolization of the thione group in ligands and subsequent replacement of hydrogen atoms by the metal ion. A significant downfield shift [CIS ($\Delta\delta$) = 0.51–0.53 ppm] (CIS = chemical-induced shift) of the azomethine ($-CH=N-$) proton signal of the complexes with respect to the corresponding free ligands confirms the coordination of the azomethine nitrogen. The signal, which is due to the $-CH_2-$ group attached

to two aromatic rings in ligands as well as in complexes, appears at nearly the same position ($\Delta\delta = 0.08\text{--}0.14$ ppm), and this suggests that the two Schiff base units remain attached in solution as well. Other resonances due to $-\text{SCH}_2-$ protons (singlet), $-\text{SCH}_3$ protons (singlet) and aromatic protons (complex multiplets) in the complexes also appear in almost the same positions as in the respective ligands. The ^1H NMR spectroscopic data are thus consistent with the ONS dibasic tridentate binding mode of each unit of ligands **I** and **II**.

^{13}C NMR Spectroscopic Studies

The ^{13}C NMR spectra recorded for complexes **3** and **4** contain ten signals that correspond to the 31 carbon atoms of the molecules and, also on account of their symmetry, the spectra for complexes **5** and **6** contain eight signals that correspond to 19 carbon atoms of the molecules. The peaks observed and their assignments are included in the Supporting Information (Tables S2 and S3), as they are compatible with the structures proposed.

^{51}V NMR Spectroscopic Studies

Complexes **3**, **4**, **5** and **6** were further characterized in solution by recording their ^{51}V NMR spectra in $[\text{D}_6]\text{DMSO}$ (see Table 3). The line widths at half-height are approximately 200 Hz. The ^{51}V NMR spectra of complexes $[\text{CH}_2\{\text{V}^{\text{VO}}_2(\text{ONS})\}_2]^{2-}$ (4 mM) in DMSO show a major resonance at $\delta = -462/-463$ ppm and a minor one at $\delta = -494/-497$ ppm. The ^{51}V nucleus is thus less shielded than commonly observed with V^{VO}_2 complexes with O,N-donor atoms. However, the chemical shifts are well within the range expected for vanadium(V) complexes where a soft S atom participates in coordination in addition to the O- and N-donor atoms.^[33]

Table 3. Summary of the ^{51}V NMR spectroscopic data and assignment of the vanadium complexes studied in this work (see text and Scheme 3).

	Chemical shifts [ppm]				
	CII	CIII	CIV	CV	CVI
3	-463.0	-495	-445	-525	-553
4	-463.0	-497	-448	-521	-553
5	-462.0	-495		-521	
6	-463.0	-495	-440	-525	

Solution Behaviour of $\text{Cs}_2[\text{CH}_2\{\text{V}^{\text{VO}}_2(\text{sal-sbdt})\}_2]\cdot 2\text{H}_2\text{O}$ (**4**)

The ^{51}V NMR spectrum of **4** dissolved in DMSO has a major resonance at $\delta = -463$ ppm and a minor one at $\delta = -495$ ppm (Figure 1a). The resonance at $\delta = -463$ ppm is assigned to $[\text{CH}_2\{\text{V}^{\text{VO}}_2(\text{sal-sbdt})(\text{Sv})\}_2]^{2-}$ (**CII**, Sv = H_2O or DMSO; Scheme 3); the two V^{VO}_2 centres are equivalent. A soft S atom participates in coordination in addition to the O and N donor atoms possibly *trans* to one of the O_{oxido}

donors, otherwise probably the peak would be detected at lower fields. The minor resonance at $\delta = -495$ ppm is tentatively assigned to species **CIII** in which the $\text{S}_{\text{thiolate}}$ is not coordinated to the V^{V} centre; the chemical shift corresponds to ONO coordination. Upon the stepwise addition of an aqueous 30% solution of H_2O_2 to the solution of **4** in DMSO (ca. 4 mM), the resonance at $\delta = -463$ ppm progressively decreases its intensity and a resonance at $\delta = -521$ ppm progressively develops (Figure 1, b–e), which we tentatively assign to $[\text{CH}_2\{\text{V}^{\text{VO}}(\text{O}_2)(\text{sal-sbdt})(\text{Sv})\}_2]^{2-}$ (**CV**; at least one of the V^{V} centres has a coordinated peroxide ligand).

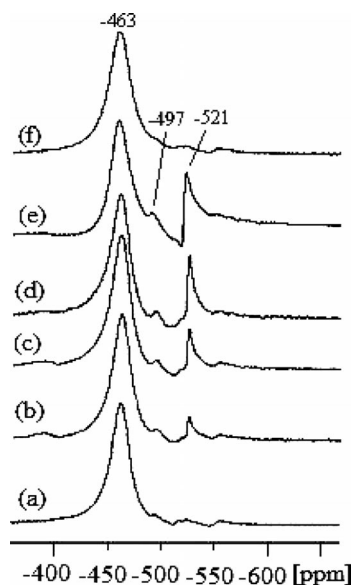


Figure 1. ^{51}V NMR spectra for solutions (ca. 4 mM) of $\text{Cs}_2[\text{CH}_2\{\text{V}^{\text{VO}}_2(\text{sal-sbdt})\}_2]\cdot 2\text{H}_2\text{O}$ (**4**): (a) in DMSO and (b–d) after stepwise additions of an aqueous solution of 30% H_2O_2 ; (b) 1.0 equiv. H_2O_2 added; (c) 2 equiv. H_2O_2 (total) added; (d) 4.0 equiv. H_2O_2 (total) added; (e) solution of (d) after leaving the tube open for 2 h; (f) solution of (e) after leaving the tube open for 36 h.

The solution that corresponds to the spectrum of Figure 1 (d) was then divided in two portions. Portion (i): The tube was left open for around 36 h. The resonance at $\delta = -521$ ppm almost disappeared, thereby indicating that, as far as V^{V} species are concerned, these were converted back to **CII**, with a signal at $\delta = -463$ ppm indicating the reversibility of the process. Additionally the ^{51}V NMR spectroscopic signals show broadening that indicates the probable presence of V^{VO} species in the solution. This was confirmed by recording the EPR spectra for both solutions (Figure 1, f, e). The spectra are reasonably intense with reasonably sharp lines, and the spin-Hamiltonian parameters obtained for the solution of Figure 1 (f) are $g_{\parallel} = 1.974$, $g_{\perp} = 1.934$, $A_{\perp} = 59 \times 10^{-4} \text{ cm}^{-1}$ and $A_{\parallel} = 178 \times 10^4 \text{ cm}^{-1}$. This indicates partial hydrolysis relative to the A_{\parallel} values expected for complex **1**.

Portion (ii): Addition of styrene resulted in the disappearance of the signal at $\delta = -521$ ppm. The only resonance clearly detected was found at $\delta = -463$ ppm, thus giving

evidence for the involvement/consumption of the peroxy species during the catalytic process.

Addition of acid (HCl, 11.6 M), that is, 1, 2, 3 and 4 equiv. to a solution of **4** (in DMSO, ca. 4 mM) led to a shift of the $\delta = -463$ ppm resonance to $\delta = -448$ ppm (see Figure 2); the solution turned red and the pH was approximately 4.5–5.0. The addition of acid might protonate the oxo group and the resonance at $\delta = -463$ ppm would progressively shift to -448 ppm (broad, ca. 98%) (Figure 2, d), which probably corresponds to an oxido/hydroxido species (**CIV**). An alternative plausible explanation for **CIV** is the protonation of one of the coordinated donor atoms of the ligand. Addition of 4 equiv. KOH to a portion of the solution of Figure 2 (d) yielded a ^{51}V NMR spectrum with a main signal at $\delta = -463$ ppm, which indicated the reversibility of the processes. The other portion was left standing and spectrum (e) was recorded.

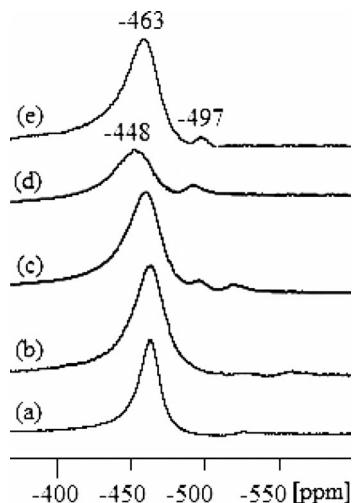
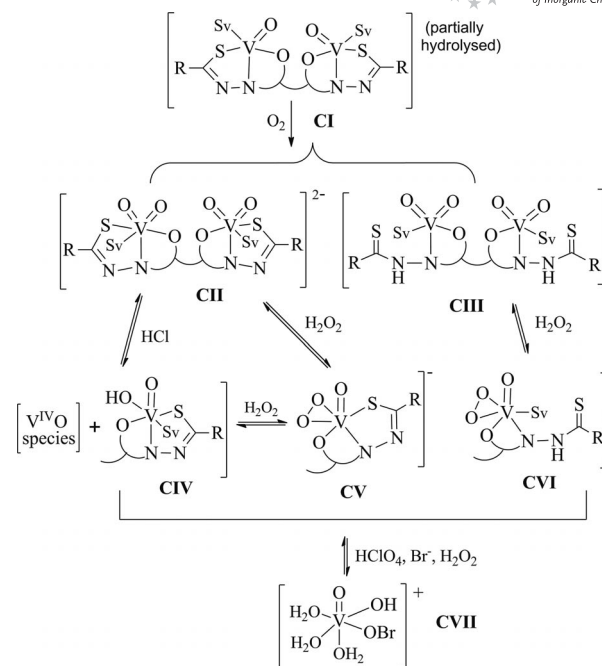


Figure 2. ^{51}V NMR spectra for solutions of $\text{Cs}_2[\text{CH}_2\{\text{VVO}_2(\text{sal-sbdt})\}_2] \cdot 2\text{H}_2\text{O}$ (**4**): (a) in DMSO (ca. 4 mM), (b) solution of (a) after addition of 1.0 equiv. of an aqueous solution of HCl (11.6 M), pH \approx 5.8; (c) solution of (b) after addition of 2.0 equiv. (total) HCl; (d) after addition of 4.0 equiv. (total) HCl (pH \approx 3.5); (e) solution of spectrum (d) after leaving the sample standing for about 24 h.

Additionally, the spectra in Figure 2 (d, e) show a broadening of the ^{51}V NMR spectroscopic signals, which indicates the probable presence of $\text{V}^{\text{IV}}\text{O}$ species in the solution. This was confirmed by recording the EPR spectra of both solutions. Both EPR spectra are reasonably intense and the spin-Hamiltonian parameters obtained are $g_{\parallel} = 1.974$, $g_{\perp} = 1.954$, $A_{\perp} = 59 \times 10^4 \text{ cm}^{-1}$ and $A_{\parallel} = 178 \times 10^4 \text{ cm}^{-1}$ for a solution of (e). The parameters are similar to those of solutions of **1** in DMSO (see below), thus indicating an O_3N or O_4 binding mode around the V^{IV} centre due to the partial reduction/hydrolysis.

Similar results were obtained in case of complexes **3**, **5** and **6** (Scheme 3). The peaks observed and their assignments are included in the Table 3 and Supporting Information (Figures S3–S7), and they are compatible with the structural formulae proposed.



Scheme 3. Summary of speciation of V^{V} -containing species in solutions of **3–6**. In **CIV**, **CV** and **CVI** either half of the V^{V} centres or both may be present as specified. For example, **CIV** might correspond to either $[\{\text{V}^{\text{V}}\text{O}_2(\text{L})(\text{Sv})\}\text{CH}_2\{\text{V}^{\text{V}}\text{O}(\text{OH})(\text{L})(\text{Sv})\}]$ or $[\{\text{V}^{\text{V}}\text{O}(\text{OH})(\text{L})(\text{Sv})\}\text{CH}_2\{\text{V}^{\text{V}}\text{O}(\text{OH})(\text{L})(\text{Sv})\}]$ (Sv = solvent). The formation of a species involving protonation of one of the coordinated donor atoms might also be a plausible assignment for **CIV**. Depending on the pH, **CVII** (a hypobromite-containing species) might include (or not) donor atoms from the ligand present in solution.

EPR and UV/Vis Studies

The EPR spectra of “frozen” solutions (77 K) in DMSO of compounds **1** and **2** are depicted in Figure 3. The lines show broadening due to both incomplete rotational averaging of the g and A tensors and probable partial precipitation of the complexes upon freezing the solutions. Apparently, two sets of lines that show hyperfine splitting due to the ^{51}V nucleus were obtained. The spectra were simulated, and the spin-Hamiltonian parameters obtained by simulation of the spectra are included in Table 4. EPR spectra were also recorded by passing He through the solutions of **1** and **2** in DMSO in the presence of ascorbic acid, but the positions of the lines remained the same.

The values of A_{\parallel} can be estimated using the additivity relationship $[A_{\parallel}^{\text{est}} = \sum A_{\parallel,i} \text{ (} i = 1 \text{ to } 4\text{)}]$ ($A_{\parallel,i}$ = contribution of each of the four donor atoms coordinated equatorially) proposed by Wüthrich^[34] and Chasteen^[35] with an estimated accuracy of $\pm 3 \times 10^4 \text{ cm}^{-1}$. The A_{\parallel} values obtained for **1** and **2** (Table 4) agree with the $A_{\parallel}^{\text{est}}$ values calculated from the partial contributions of the equatorial donor groups^[29,32,35–37] relevant in the present case [H_2O ($45.7 \times 10^4 \text{ cm}^{-1}$), $\text{O}_{\text{phenolate}}$ ($38.9 \times 10^4 \text{ cm}^{-1}$), N_{imine} (38.1 to $43.7 \times 10^4 \text{ cm}^{-1}$), O_{DMSO} ($41.9 \times 10^4 \text{ cm}^{-1}$), $\text{S}_{\text{thiolate}}$ ($31.9 \times 10^4 \text{ cm}^{-1}$)] either assuming an NO_3 (species II) or

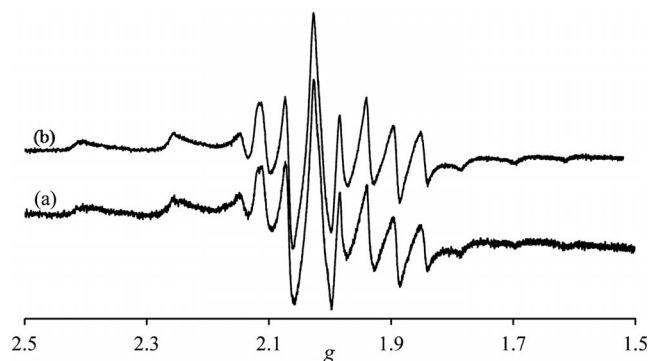


Figure 3. First-derivative EPR spectra of frozen (77 K) solutions (ca. 4 mM) (a) $[\text{CH}_2\{\text{V}^{\text{IVO}}(\text{sal-sbdt})(\text{H}_2\text{O})\}_2]$ (**1**) in DMSO (b) $[\text{CH}_2\{\text{V}^{\text{IVO}}(\text{sal-smtdt})(\text{H}_2\text{O})\}_2]$ (**2**) in DMSO. The solutions were frozen after around 15 min of mixing of the solid and solvent.

Table 4. Spin-Hamiltonian parameters obtained by simulation^[38] of the experimental first-derivative EPR spectra recorded for solutions of complexes **1** and **2** in DMSO at 77 K.

Complexes (5 mM, DMSO)		g_{\parallel}	A_{\parallel} [$\times 10^{-4} \text{ cm}^{-1}$]	g_{\perp}	A_{\perp} [$\times 10^{-4} \text{ cm}^{-1}$]
1	species I	1.936	178.1	1.976	65.0
	species II	1.942	164.9	1.977	64.9
2	species I	1.937	177.4	1.976	65.1
	species II	1.942	165.4	1.976	65.2

an O_4 (species I) equatorial binding set. If $\text{S}_{\text{thiolate}}$ is considered to be an equatorial donor atom, the $A_{\parallel}^{\text{est}}$ are much lower (ca. $157 \times 10^{-4} \text{ cm}^{-1}$). Thus, at least in DMSO solution the $\text{S}_{\text{thiolate}}$ is not bound to the V^{IV} centre (at least equatorially).

Addition of 1, 2 and 3 equiv. H_2O_2 to solutions of **1** or **2** in DMSO acidifies the solutions, and V^{IVO} species form (see Figure 4) with almost identical spin-Hamiltonian parameters ($g_{\parallel} = 1.939$, $A_{\parallel} = 177.8 \times 10^{-4} \text{ cm}^{-1}$ for **1**; and $g_{\parallel} = 1.935$, $A_{\parallel} = 178.0 \times 10^{-4} \text{ cm}^{-1}$ for **2**). The V^{IVO} is also progressively oxidized to V^{V} . According to the g_{\parallel} and A_{\parallel} values obtained for these partially oxidized solutions, in these V^{IVO} species the equatorial binding set is probably O_4 , thus indicating the substitution of donor atoms of the ligand by DMSO and/or H_2O molecules in the coordination sphere.

The EPR spectra thus indicate that upon dissolving **1** in DMSO, the V^{IV} complex partly hydrolyzes and oxidizes; in solution the binding set ($\text{O}_{\text{phenolate}}$, N_{imine} , $\text{S}_{\text{thiolate}}$, $\text{O}_{\text{water/equatorial}}$) is not detected by EPR for the V^{IVO} complexes formed upon dissolution. The ^{51}V NMR spectrum of this solution depicts a resonance at $\delta = -463$ ppm (Figure 5a). The resonance at $\delta = -463$ ppm is assigned to $[\text{CH}_2\{\text{V}^{\text{VO}}_2(\text{sal-sbdt})(\text{Sv})\}_2]^{2-}$ (**CII**, $\text{S} = \text{H}_2\text{O}$ or DMSO Scheme 3). Typically, the ^{51}V NMR spectra of the solutions of either complex **1** or **2** were measured after approximately 1 h of mixture of the solids with the solvent. Upon the stepwise addition of an aqueous 30% solution of H_2O_2 to the solution of **3** (in DMSO, ca. 4 mM), the resonance at $\delta = -520$ ppm appears. It corresponds to the mono-peroxo species.

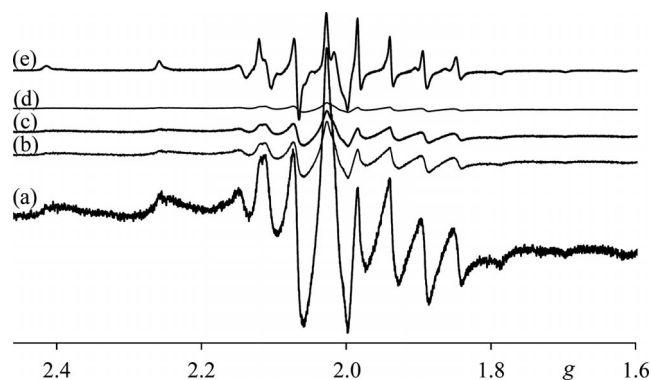


Figure 4. First-derivative EPR spectra of 4 mM $[\text{CH}_2\{\text{V}^{\text{IVO}}(\text{sal-sbdt})(\text{H}_2\text{O})\}_2]$ (**1**) (a) in DMSO; (b) after addition of 1.0 equiv. of H_2O_2 (aqueous 30% solution), (c) after addition of a total of 2.0 equiv. of H_2O_2 , (d) after addition of a total of 3.0 equiv. of H_2O_2 and (e) after addition of a total of 10 equiv. of styrene to the solution of (d).

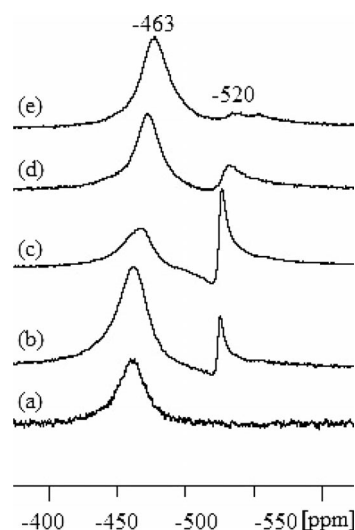


Figure 5. ^{51}V NMR spectra for solutions (ca. 4 mM) of complex $[\text{CH}_2\{\text{V}^{\text{IVO}}(\text{sal-sbdt})(\text{H}_2\text{O})\}_2]$ (**1**) (a) in DMSO and (b–d) after stepwise additions of an aqueous solution of 30% H_2O_2 : (b) 1.0 equiv. H_2O_2 added, (c) 2 equiv. H_2O_2 (total) added, (d) 4.0 equiv. H_2O_2 (total) added and (e) solution of (d) after the addition of 10 equiv. of styrene.

Similar changes in the EPR and ^{51}V NMR spectra have also been observed for solutions of complex **2** (4 mM) in DMSO upon addition of H_2O_2 . The spectra recorded are presented in the Supporting Information (Figures S8 and S9).

The formation of peroxo complexes in methanol by treatment of **1** and **2** with H_2O_2 was also studied by electronic absorption spectroscopy. Thus, the addition of two drops of a dilute solution of H_2O_2 (3.21 g, 28.3 mmol of 30% aqueous H_2O_2 dissolved in 30 mL of MeOH) to a $6.43 \times 10^{-5} \text{ M}$ solution of **1** in methanol (ca. 20 mL) and recording the spectra after every 15 min interval resulted in the spectral changes presented in Figure 6. The band at 417 nm slightly decreases in intensity and the λ_{max} slowly shifts to 400 nm. Simultaneously, the weak shoulder that

appears at approximately 350 nm slowly sharpens with a slight gain in intensity. The band at 297 nm gains intensity while maintaining the position, and bands at 210 and 240 nm sharply gain intensity. The three d-d bands that appear at 575, 680 and 845 nm (in **1**) and at 565, 675 and 875 nm (in **2**) recorded with more concentrated solutions slowly decrease their intensities and finally become indistinguishable (Figure 7). Changes in the UV/Vis spectra similar to those presented here have been interpreted as involving the progressive oxidation of $V^{IV}O$ species followed by formation of a oxidoperoxovanadium(V) compound.^[17,39] However, peroxo-to-vanadium charge-transfer transitions have been reported at $\lambda_{\max} \approx 450$ nm.^[40] In the present systems, the electronic spectra of both complexes exhibit rather strong broad bands at approximately 410 nm, probably involving the C=N group,^[37,41] thus in the same range of the peroxo-to-vanadium charge-transfer transition, which makes the detection of the latter band difficult. It is possible that there are several processes taking place, namely, the

formation of species **CV** and **CVI**, which decrease the contribution of the band that involves the C=N group and precludes the observation of an increase in the absorption around 400–450 nm.

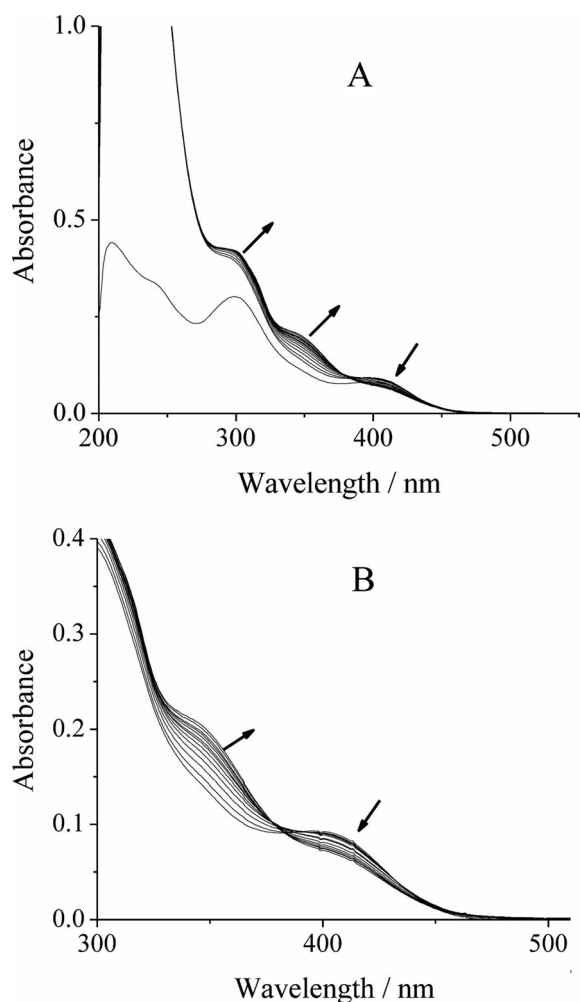


Figure 6. Spectral changes obtained after adding two drops of a dilute aqueous/MeOH solution of H_2O_2 (3.21 g, 28.3 mmol 30% aqueous H_2O_2 dissolved in 30 mL of MeOH) to a solution of $[CH_2\{V^{IV}O(sal-sbdt)(H_2O)\}_2]$ (**1**) in methanol (ca. 6.43×10^{-5} M, 20 mL). The spectra were recorded every 15 min. The expanded region of 300 to 500 nm is shown in B.

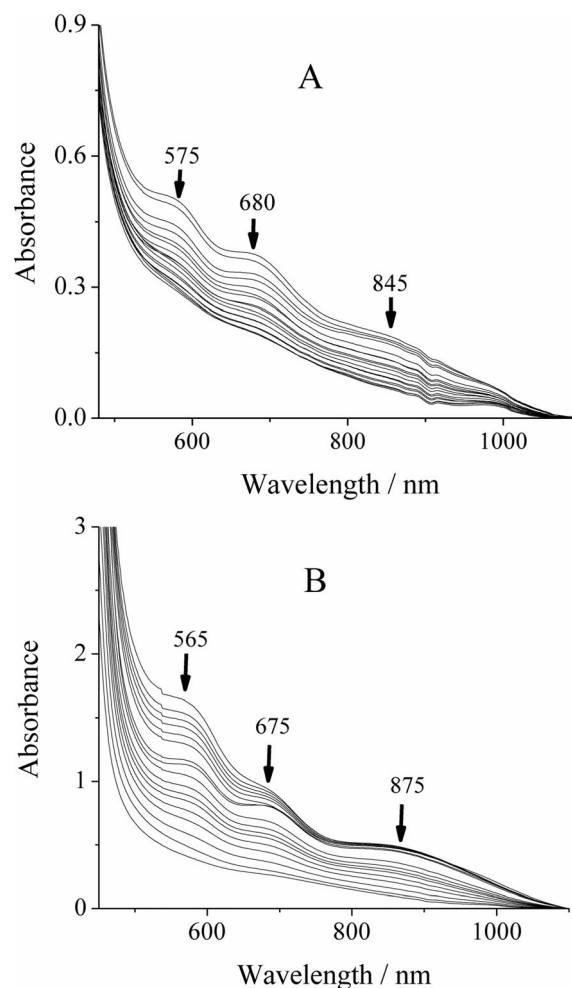


Figure 7. Spectral changes obtained during titration of (A) 20 mL of a 5.76×10^{-3} M solution of $[CH_2\{V^{IV}O(sal-sbdt)(H_2O)\}_2]$ (**1**) in DMSO, (B) 20 mL of a 8.76×10^{-3} M solution of $[CH_2\{V^{IV}O(sal-smtd)(H_2O)\}_2]$ (**2**) in DMSO, with a dilute solution of H_2O_2 (1.26 g, 11.1 mmol of 30% aqueous H_2O_2 in 5 mL of DMSO). The spectra were recorded after the successive addition of one-drop portions, at 2 min time intervals. The three d-d bands recorded progressively decrease their intensity as $V^{IV}O$ complexes are oxidized to V^V species.

Similar changes in the UV region of the absorption spectra of **2** could also be observed when using lower concentrations (Figure S10 in the Supporting Information). Thus, addition of two drops of a dilute aqueous/MeOH solution of H_2O_2 (3.21 g, 28.46 mmol of 30% aqueous H_2O_2 dissolved in 30 mL of MeOH) to a 6.33×10^{-5} M solution of $[CH_2\{V^{IV}O(sal-smtd)(H_2O)\}_2]$ in methanol (20 mL) yielded an increase in the intensity of the band at 215 nm, along with only a small gain in the intensity of the 305 nm band with a marginal shift towards a lower wavenumber. Further additions of H_2O_2 resulted in the slow decrease in intensity of the 405 nm band along with broadening, whereas the weak shoulder that appeared at approximately 350 nm

slowly sharpened with a slight gain in intensity. The 215 and 305 nm bands only showed a marginal increase in intensity.

The reactivity of $\text{Cs}_2[\text{CH}_2\{\text{V}^{\text{VO}}_2(\text{sal-sbdt})\}_2]\cdot 2\text{H}_2\text{O}$ (**4**) and $\text{Cs}_2[\text{CH}_2\{\text{V}^{\text{VO}}_2(\text{sal-smtdt})\}_2]\cdot 2\text{H}_2\text{O}$ (**6**) with H_2O_2 was also tested and spectral changes were monitored by electronic absorption spectroscopy. The spectral changes obtained upon adding successive one-drop portions of an aqueous/MeOH solution of H_2O_2 (3.21 g, 28.3 mmol of 30% aqueous H_2O_2 dissolved in 30 mL of MeOH) to a solution of **4** in methanol (ca. 5.63×10^{-5} M, 20 mL) are presented in Figure S11 in the Supporting Information. A considerable increase in the intensity of the 210 nm band and an increase in the intensity of the 297 nm band was observed at the beginning (i.e., after addition of about 20 drops of H_2O_2), whereas the band at 410 nm remained nearly constant. Upon further addition of H_2O_2 , the weak shoulder that appeared at around 345 nm started to emerge, along with weakening of the band at around 410 nm (Figure S11). Similar spectral changes were obtained for **6** (Figure S12 in the Supporting Information). The final spectra in both cases were similar to those obtained by the reaction of the corresponding $\text{V}^{\text{IV}}\text{O}$ complexes with H_2O_2 .

The behaviour of the solutions of the V^{VO}_2 complexes in methanol upon addition of HCl was also monitored by electronic absorption spectroscopy. Thus the dropwise addition of HCl dissolved in methanol (3.9×10^{-3} M) to a solution of $\text{Cs}_2[\text{CH}_2\{\text{V}^{\text{VO}}_2(\text{sal-sbdt})\}_2]\cdot 2\text{H}_2\text{O}$ (**4**) (ca. 2.85×10^{-5} M, 20 mL) caused the darkening of the solution along with slow broadening of bands. The spectral changes are depicted in Figure 8.

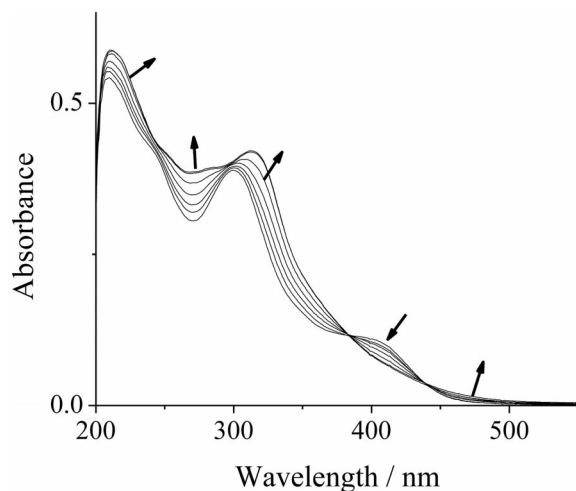
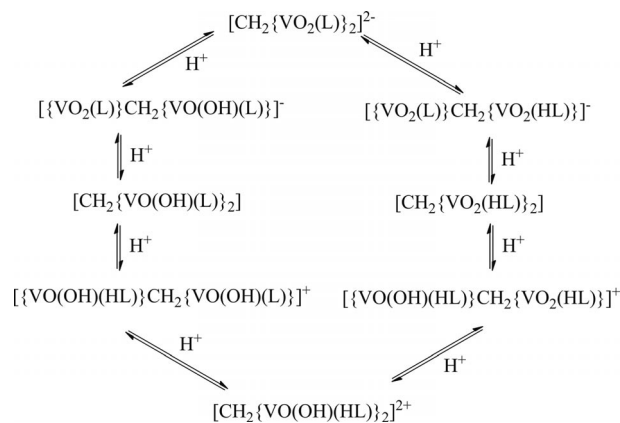


Figure 8. Spectral changes obtained during titration of a 2.85×10^{-5} M solution of $\text{Cs}_2[\text{CH}_2\{\text{V}^{\text{VO}}_2(\text{sal-sbdt})\}_2]\cdot 2\text{H}_2\text{O}$ (**4**) in methanol (20 mL) upon dropwise additions of HCl dissolved in MeOH (3.9×10^{-3} M). Each spectrum was recorded upon successive additions of one-drop portions.

Very similar features were also observed with solutions of **3**, **5** and **6**. The spectral changes in the case of $\text{Cs}_2[\text{CH}_2\{\text{V}^{\text{VO}}_2(\text{sal-smtdt})\}_2]\cdot 2\text{H}_2\text{O}$ (**6**) are presented in Figure S13 in the Supporting Information.

As reported for other systems,^[29,40,42] besides the formation of V^{IV} species, we interpret these results by assuming the formation of oxidohydroxido species with the formula $[\text{CH}_2\{\text{V}^{\text{VO}}(\text{OH})(\text{HL})\}_2]^{2+}$ via $[\text{CH}_2\{\text{V}^{\text{VO}}_2(\text{HL})\}_2]$ and/or $[\text{CH}_2\{\text{V}^{\text{VO}}_2(\text{OH})(\text{HL})\}_2]$ (see Scheme 4). It is also possible that complexes $[\text{CH}_2\{\text{VO}_2(\text{HL})(\text{Sv})\}_2]$ might also form. Protonation of the hydrazone nitrogen has been reported {e.g., for the structurally characterized $[\text{VO}(\text{Hsal-bhz})]$ ($\text{H}_2\text{sal-bhz}$ derives from salicylaldehyde and benzoylhydrazide)}, which forms upon treatment of the corresponding anionic dioxido complex with HCl.^[43] EPR and electron spin echo envelope modulation (ESEEM) spectra recorded for $[\text{VO}(\text{salim})(\text{acac})]$ (salim = a Schiff base ligand that contains imidazole) upon addition of acid were explained by the protonation of the imine N atom.^[44] Very similar results were obtained for related binucleating ligands^[29] that involve an ONO binding set and were interpreted similarly. Scheme 4 may be considered to summarize the processes that take place, with one of the =N–N= nitro- gen atoms being the site of protonation.



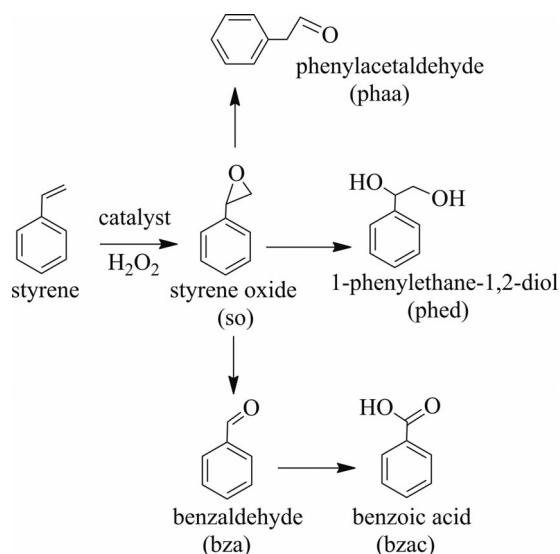
Scheme 4. Formation of $[\text{CH}_2\{\text{V}^{\text{VO}}(\text{OH})(\text{HL})\}_2]^{2+}$ by successive protonations starting with complexes $[\text{CH}_2\{\text{V}^{\text{VO}}_2(\text{L})\}_2]^{2-}$. All included species are in equilibria. Each $\text{V}^{\text{VO}}_2(\text{L})$, $\text{V}^{\text{VO}}_2(\text{HL})$, $\text{V}^{\text{VO}}(\text{OH})(\text{L})$ and $\text{V}^{\text{VO}}(\text{OH})(\text{HL})$ core will probably correspond to a different chemical shift in the ^{51}V NMR spectra.

Catalytic Activity

Oxidation of Styrene

Oxidation of styrene has been reported by several researchers using homogeneous as well as heterogeneous catalysts, and the major oxidation products obtained are styrene oxide, benzaldehyde, benzoic acid, phenylacetaldehyde and 1-phenylethane-1,2-diol (Scheme 5).^[12,39a,45] We carried out the oxidation of styrene using $\text{Cs}_2[\text{CH}_2\{\text{V}^{\text{VO}}_2(\text{sal-sbdt})\}_2]\cdot 2\text{H}_2\text{O}$ (**4**) and $\text{Cs}_2[\text{CH}_2\{\text{V}^{\text{VO}}_2(\text{sal-smtdt})\}_2]\cdot 2\text{H}_2\text{O}$ (**6**) as catalyst precursors and using an aqueous hydrogen peroxide solution as oxidant. All these expected products were obtained as well as minor amounts of unidentified products.

The following parameters were studied by taking $\text{Cs}_2[\text{CH}_2\{\text{V}^{\text{VO}}_2(\text{sal-smtdt})\}_2]\cdot 2\text{H}_2\text{O}$ (**6**) as a representative catalyst precursor with the objective being to obtain the maximum oxidation of styrene: (i) amount of catalyst, (ii) amount of oxidant and (iii) amount of solvent.



Scheme 5. Various oxidation products of styrene obtained and identified in the catalytic reactions reported in this work.

The effect of the amount of catalyst on the oxidation of styrene was studied as a function of time and the results are presented in Figure 9 (a). Three different amounts of **6**,

namely, 0.0010, 0.0035 and 0.0050 g, were used with a styrene (10 mmol)/aqueous 30% H_2O_2 molar ratio of 1:1 dissolved in methanol (5 mL), and the reaction was carried out at 80 °C. As shown in Figure 9, 0.0010 g of **6** gave 99% conversion of styrene in 8 h of reaction time. Increasing the amount of catalyst precursor lowered the conversion. Thus, 0.0010 g of catalyst may be considered sufficient to run the reaction under the above conditions. Variable solubility of the catalyst in limited methanol is possibly the reason for less conversion of substrate with a higher amount of catalyst.

Similarly, three different molar ratios of aqueous 30% H_2O_2 to styrene (e.g., 1:0.5, 1:1 and 1:2) were considered under similar reaction conditions (i.e., 0.0010 g of **6** in 5 mL of methanol and carrying out the reaction at 80 °C for 8 h). The increase in the H_2O_2 -to-styrene ratio from 1:0.5 to 1:1 improved the conversion from 66 to 99%, whereas the 1:2 ratio did not significantly improve the conversion (Figure 9, b). The volume of solvent also affected the net conversion of styrene. Thus, varying the methanol amount from 5 to 7 mL improved the rate of conversion and the reaction acquired a steady state in a shorter period of time, though it did not affect the overall conversion of styrene (Figure 9, c). When using 10 mL of methanol, the reaction took longer to acquire the steady state, probably due to dilution of the reactants.

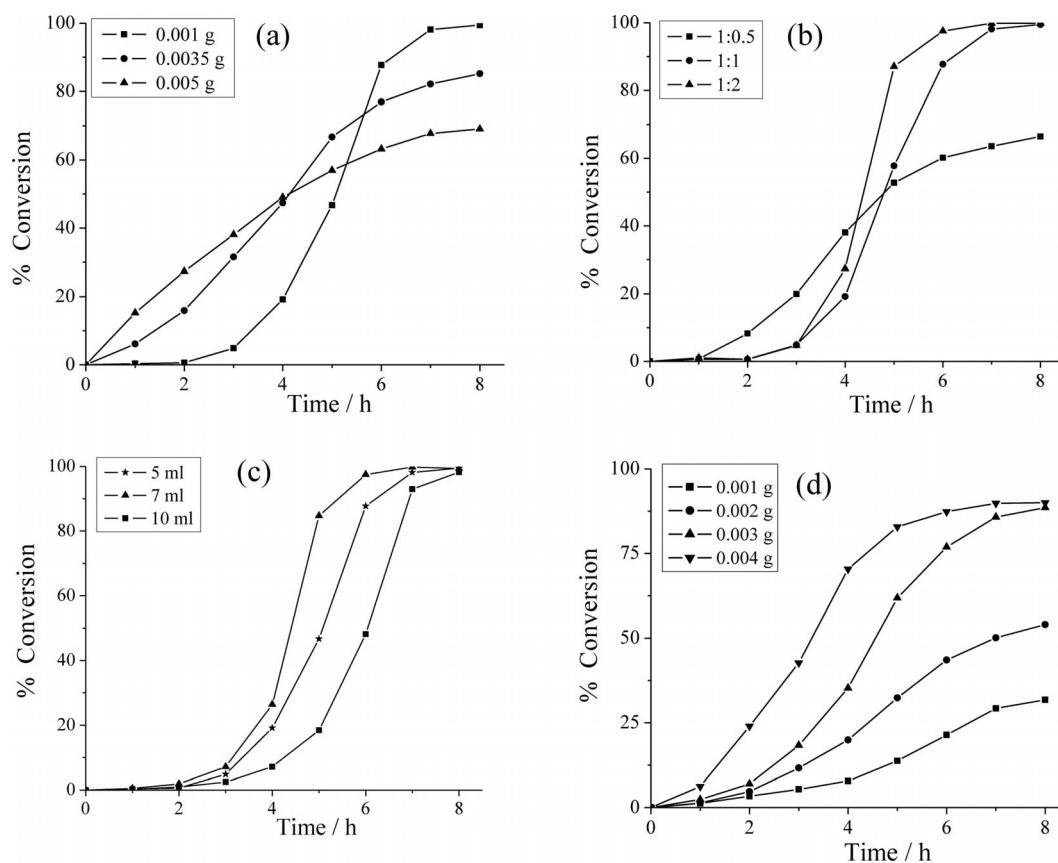


Figure 9. (a) Effect of the amount of catalyst on the oxidation of styrene. (b) Effect of H_2O_2 amount (H_2O_2 /styrene molar ratio) on oxidation of styrene. (c) Effect of volume of solvent (methanol) on the oxidation of styrene. (d) Effect of amount of catalyst precursor, $\text{Cs}_2[\text{CH}_2\{\text{V}^{\text{VO}}_2(\text{sal-sbd})\}_2] \cdot 2\text{H}_2\text{O}$ (**4**), on the oxidation of styrene. For reaction conditions, see text.

After setting the optimized reaction conditions (i.e., 10 mmol of styrene, 10 mmol of 30% H₂O₂ and 0.0010 g of catalyst in 7 mL of methanol at 80 °C) for **6**, another catalyst precursor, **4**, was also tested under the same reaction conditions. Thus, 10 mmol of styrene, 10 mmol of 30% H₂O₂ and 0.0010 g of **4** were dissolved in methanol (7 mL) and the reaction was carried out at 80 °C. A maximum of around 32% conversion was only obtained after 8 h of reaction time. However, by increasing the amount of **4** the conversion also increased, and as high as 88% conversion of styrene was achieved with 0.0030 g of catalyst in 8 h of reaction time. The reaction was completed in approximately 5 h upon increasing the amount of **4** to 0.0040 g, but the final conversion is almost same (90%) (Figure 9, d). The conversion and selectivity of different products are presented in Table 5. Thus, the performance of catalyst precursor **6** is much better (TOF = 1148 h⁻¹) relative to **4** (TOF = 396 h⁻¹). A blank reaction under the above conditions gave approximately 3% conversion of styrene.

Table 5. Product selectivity and percent conversion of styrene after 8 h of reaction time.

Cat.	Conv. [%]	TOF [h ⁻¹] ^[a]	Selectivity [%] ^[b]					
			so	Bza	Phed	bzac	phaa	other
4	88	396	4.4	10.8	40.3	30.4	13.8	0.3
6	99	1148	3.7	4.6	11.2	77.2	3.0	0.3
7	56	308	6	15	22	36	9	12
8	60	274	7	14	20	37	9	13

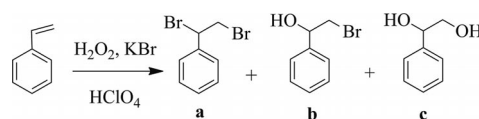
[a] Higher TOF for catalyst **6** is due to its better performance (with lower amount) in catalytic reaction. [b] so: styrene oxide, bza: benzaldehyde, phed: 1-phenylethane-1,2-diol, bzac: benzoic acid, phaa: phenylacetaldehyde.

From Table 5 it is clear that both the turnover frequency (TOF) and selectivity values presented differ significantly for both complexes, and that Cs₂[CH₂{VO₂(sal-smdt)}₂·2H₂O has excellent catalytic activity for the oxidation of styrene, with benzoic acid being the more important product. Under the optimized reaction conditions for maximum conversion of styrene, the selectivity of the products formed using **4** as catalyst precursor follows the order 1-phenylethane-1,2-diol > benzoic acid > phenylacetaldehyde > benzaldehyde > styrene oxide, whereas in case of **6** the order is benzoic acid > 1-phenylethane-1,2-diol > benzaldehyde > styrene oxide > phenylacetaldehyde. Formation of styrene (ep)oxide in low amount indicates its conversion to other products. Indeed the experimental conditions were not optimized for the formation of the epoxide.

We have also obtained the oxidation of styrene by using 0.0010 g each of the corresponding mononuclear complexes K[V^{VO}₂(sal-sbdt)(H₂O)] (**7**) and Na[V^{VO}₂(sal-smdt)(H₂O)] (**8**) and the results are also presented in Table 5. It is clear from the table that both show catalytic activity but binuclear complexes are more active than their corresponding mononuclear complexes. In fact, the complexes reported here perform much better than several other reported vanadium compounds.^[6c]

Oxidative Bromination of Styrene

Oxidative bromination of styrene under a two-phase system by using Cs₂[CH₂{VO^V(sal-sbdt)}₂·2H₂O and Cs₂[CH₂{VO^V(sal-smdt)}₂·2H₂O as catalyst precursors in the presence of KBr, HClO₄ and H₂O₂ gave mainly three products, namely, (a) 1,2-dibromo-1-phenylethane, (b) 2-bromo-1-phenylethane-1-ol and (c) 1-phenylethane-1,2-diol (Scheme 6). Some minor products (benzaldehyde, styrene epoxide, benzoic acid and 4-bromostyrene) were also detected but their overall percentage is approximately 7% of the total of the main products. The obtained products are the same as those reported by Conte et al.^[5,6a] Addition of HClO₄ in four equal portions was required to obtain better oxidative bromination. All products were separated/isolated by column chromatography and the content of each fraction was confirmed by ¹H NMR spectroscopy as well as GC-MS.



Scheme 6. Main products obtained by oxidative bromination of styrene: (a) 1,2-dibromo-1-phenylethane (dibromide), (b) 2-bromo-1-phenylethane-1-ol (a bromohydrin) and (c) 1-phenylethane-1,2-diol.

The following parameters were studied to optimize the reaction conditions for the maximum oxidative bromination of styrene by taking **6** as catalyst precursor: (i) catalyst amount, (ii) oxidant amount and (iii) catalyst precursor.

Three different amounts of **6** (0.0010, 0.0020 and 0.0030 g) were used as catalyst precursor while keeping fixed the amounts of styrene (1.04 g, 10 mmol), KBr (4.76 g, 40 mmol), 30% H₂O₂ (6.81 g, 60 mmol) and aqueous 70% HClO₄ (5.72 g, 40 mmol) in a CH₂Cl₂/water (50% v/v) mixture (40 mL) at room temperature. As presented in Figure 10 (a), a maximum of 99% conversion was obtained after 1 h of reaction with 0.0010 g of catalyst precursor, and 0.0020 and 0.0030 g of catalyst precursor gave nearly the same conversion. Therefore, 0.0010 g of **6** was set as optimum. Additions of HClO₄ were made in four portions, one immediately after the catalyst precursor (reaction time = 0) and the three other portions with 15 min intervals.

To optimize the amount of HClO₄, three different amounts of 70% HClO₄ were used for fixed amounts of styrene (1.04 g, 10 mmol), catalyst precursor (0.0010 g), KBr (4.76 g, 40 mmol), 30% H₂O₂ (6.81 g, 60 mmol) and CH₂Cl₂/H₂O (40 mL, 50% v/v) at room temperature for 1 h. Increasing the perchloric acid amount from 1.43 g (10 mmol) to 2.86 g (20 mmol) increased the conversion from 61 to 99%. Only a slight improvement in conversion was obtained upon further increasing this amount to 4.29 g (30 mmol). Therefore, 2.86 g of 70% HClO₄ was considered to be the more adequate one (Figure 10, b), thus making additions in four equal portions.

The effect of the amount of H₂O₂, added as an aqueous 30% H₂O₂ solution, was studied with substrate-to-oxidant

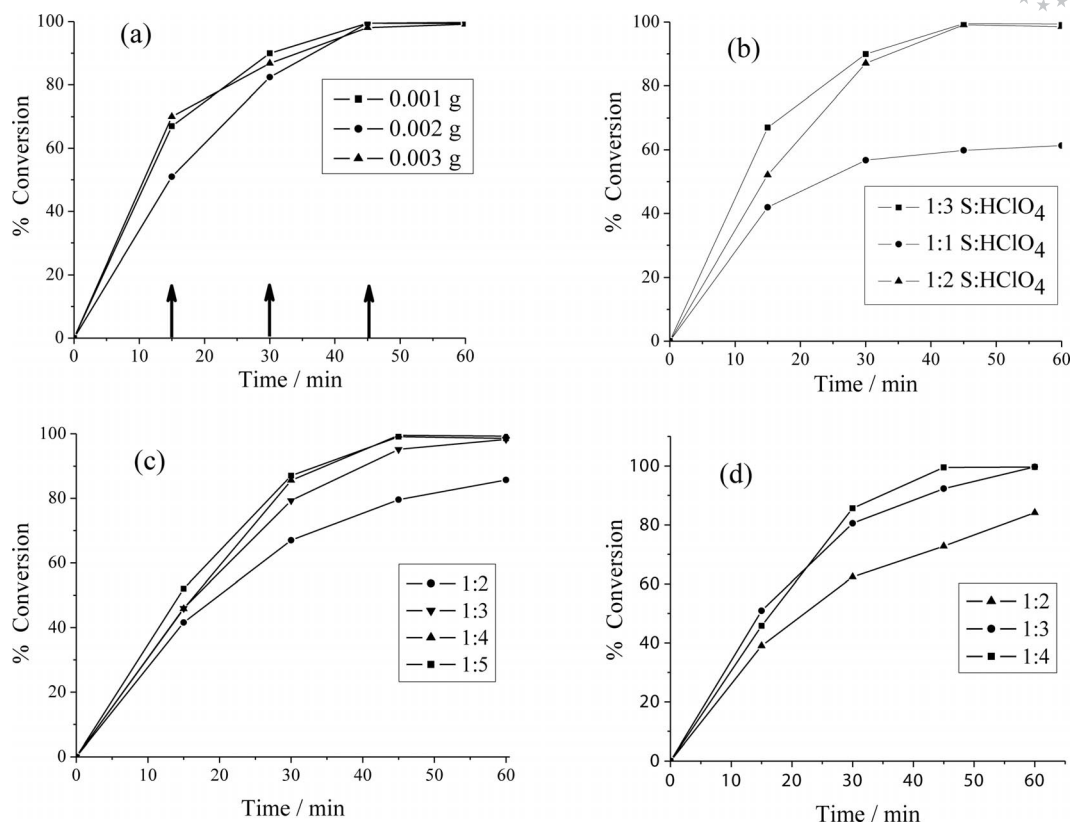


Figure 10. (a) Effect of catalyst amount on oxidative bromination of styrene. Reaction conditions: styrene (1.04 g, 10 mmol), amount of catalyst precursor (0.0010, 0.0020 or 0.0030 g), KBr (4.76 g, 40 mmol), aqueous 30% H_2O_2 (6.81 g, 60 mmol) and 70% HClO_4 (5.72 g, 40 mmol) added in four equal portions at $t = 0, 15, 30$ and 45 min of reaction time (marked with arrows in the figure), and $\text{CH}_2\text{Cl}_2/\text{H}_2\text{O}$ (40 mL, 50% v/v) at room temperature for 1 h. (b) Effect of the amount of perchloric acid, added in four equal portions in 15 min intervals, on the oxidative bromination of styrene. (c) Effect of the amount of H_2O_2 on the oxidative bromination of styrene. (d) Effect of the amount of KBr on the oxidative bromination of styrene. See text for other conditions for plots (b), (c) and (d).

ratios of 1:2, 1:3, 1:4 and 1:5 for a fixed amount of styrene (1.04 g, 10 mmol), amount of catalyst precursor (0.0010 g), KBr (4.76 g, 40 mmol) and HClO_4 (2.86 g, 20 mmol) in $\text{CH}_2\text{Cl}_2/\text{H}_2\text{O}$ (40 mL, 50% v/v), and the reaction was monitored at room temperature for 1 h. The conversion increased upon increasing the substrate-to-oxidant ratio, and a 1:3 ratio was sufficient to convert 98% styrene. Increasing this ratio further did not improve the final conversion, except to complete the reaction in a shorter time (ca. 50 min; Figure 10, c).

Similarly, three different substrate-to-KBr ratios were used. Upon increasing the amount of KBr from 1:2 to 1:3, the obtained conversion increased from approximately 84 to 99%, but a further increase in the KBr amount gave almost the same conversion (Figure 10, d).

Table S4 in the Supporting Information summarizes all conditions applied to optimize the reaction conditions for the maximum oxidative bromination of styrene when using **6** as catalyst precursor. Entry 10 of this table presents the optimized reaction conditions, which are styrene (1.04 g, 10 mmol), amount of catalyst precursor 0.0010 g, 30% aqueous H_2O_2 (3.40 g, 30 mmol), 3.56 g (30 mmol) of KBr, HClO_4 (2.86 g, 20 mmol) added in four equal portions in 15 min intervals, and $\text{CH}_2\text{Cl}_2/\text{H}_2\text{O}$ (40 mL, 50% v/v) at room temperature for 1 h. Figure 11 represents the con-

sumption of styrene and the selectivity of the formation of major products with time for these experimental conditions.

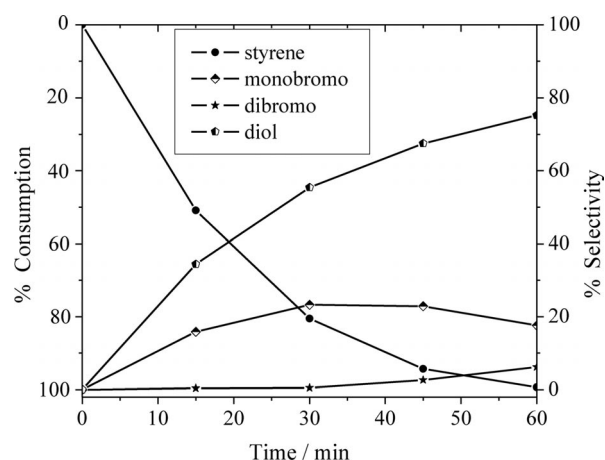


Figure 11. Percentage consumption of styrene and selectivity of the formation of products with time using $\text{Cs}_2[\text{CH}_2\{\text{VO}^{\text{V}}(\text{sal-smdt})\}_2] \cdot 2\text{H}_2\text{O}$ (**6**) as catalyst precursor and the optimized conditions specified in the text.

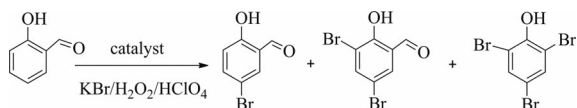
The formation of all three products starts with the consumption of styrene. However, among the three products formed, the selectivity of 1-phenylethane-1,2-diol reaches

75% at the end of 1 h, whereas that of 1,2-dibromo-1-phenylethane is only 6%. The selectivity of the formation of 2-bromo-1-phenylethane-1-ol (bromohydrin) initially increases, reaching approximately 23%, and after around 40 min of reaction decreases. It is around 18% at the end of 1 h. Increasing the reaction time beyond 1 h increased the formation of the dibromide but decreased that of the bromohydrin, whereas 1-phenylethane-1,2-diol remained almost constant. It should be noted here that for the catalytic oxidation of styrene the experimental conditions were set up for maximum conversion of styrene, and the product obtained in higher relative amounts was 1-phenylethane-1,2-diol, not the bromohydrin.

We have also obtained oxidative bromination of styrene by using mononuclear complexes $K[VVO_2(\text{sal-sbdt})(H_2O)]$ (**7**) and $Na[VVO_2(\text{sal-smdt})(H_2O)_2]$ (**8**) (0.0010 g of each) under the above optimized conditions. Conversions obtained after 1 h of reaction time were 98 and 97%, respectively. Using 0.0010 g of mononuclear complexes approximately corresponded to the same number of moles of metal centres as for binuclear complexes; hence their catalytic potential is almost the same as that of the binuclear complexes.

Oxidative Bromination of Salicylaldehyde

Vanadium(V) complexes also catalyze the oxidative bromination of salicylaldehyde in the presence of H_2O_2 . In the present study, complexes **3–6** were used as catalyst precursors with water as solvent. The catalytic oxidative bromination of salicylaldehyde gave 5-bromosalicylaldehyde, 3,5-dibromosalicylaldehyde and 2,4,6-tribromophenol (Scheme 7). These were the same products obtained when using related VVO_2 complexes of ONO donor ligands.^[29] After several trials, the optimized reaction conditions for maximum conversion of salicylaldehyde were obtained. These were salicylaldehyde (2.44 g, 20 mmol), KBr (5.95 g, 50 mmol), aqueous 30% H_2O_2 (15.0 g, 120 mmol), catalyst precursor (0.0070 g of **4**, 0.0060 g of **6**, 0.0060 g of **3** and 0.0050 g of **5**), aqueous 70% $HClO_4$ (4.02 g, 80 mmol) and water (40 mL). It was observed that the addition of $HClO_4$ in four distinct portions during the first two hours was necessary to obtain a better conversion. The conversion of salicylaldehyde and the selectivity toward different products after 7 h of reaction time are presented in Table 6.



Scheme 7. Products obtained upon the catalytic oxidative bromination of salicylaldehyde using complexes **3–6** as catalyst precursors and water as solvent.

From the table it may be observed that with the catalyst precursor **6** and with a substrate-to- H_2O_2 molar ratio of 1:2, approximately 89% conversion was achieved with highest selectivity towards the formation of 5-bromosalicylaldehyde (81.3%), followed by the formation of 3,5-dibromosal-

Table 6. Results of oxidative bromination of salicylaldehyde catalyzed by **3–8**. Conversion and relative amounts of products obtained after 7 h of reaction.

Entry	Catalyst precursor	Substr. / H_2O_2	Conv. [%]	TOF [h^{-1}]	Selectivity of product		
					mono	dibromo	tribromo
1	6	1:2	89	393	81.3	17.4	1.3
2	6	1:3	87	386	76.2	21.9	1.9
3	6	1:4	88	388	68.4	28.5	3.1
4	6	1:5	88	390	55.2	39.6	5.2
5	6	1:6	89	391	40.3	51.8	7.9
6	5	1:6	86	365	38.8	59.3	6.9
7	4	1:6	91	403	36.2	55.3	8.5
8	3	1:6	89	378	28.8	61.4	9.8
9	7	1:6	98	176	33	66	1
10	8	1:6	99	172	34	65	1

icylaldehyde (17.4%); only about 1.3% of 2,4,6-tribromophenol was formed. Increasing the H_2O_2 /substrate molar ratio did not improve the conversion of salicylaldehyde significantly, but the degree of bromination of the substrate increased (i.e., the degree of formation of 3,5-dibromosalicylaldehyde and 2,4,6-tribromophenol was significantly higher). The corresponding mononuclear complexes $K[VVO_2(\text{sal-sbdt})(H_2O)]$ (**7**) and $Na[VVO_2(\text{sal-smdt})(H_2O)_2]$ (**8**) exhibited 98 and 99% conversion, respectively, with 65 and 66% selectivity towards major product 3,5-dibromosalicylaldehyde. A maximum of 54 and 50% conversion of salicylaldehyde with 87 and 85% selectivity, respectively, was reported with mononuclear complexes $K[VO_2(\text{sal-inh})\cdot H_2O]$ and $K[VO_2(\text{sal-bhz})\cdot H_2O]$.^[46]

The catalytic potential of these complexes in the oxidative bromination of salicylaldehyde also compares well with similar binuclear complexes that have ONO-donor ligands. For example, complexes $K_2[CH_2\{VO^V(\text{sal-nah})\}_2]\cdot 2H_2O$, $K_2[CH_2\{VO^V(\text{sal-bhz})\}_2]\cdot 2H_2O$, $K_2[CH_2\{VO^V(\text{sal-fah})\}_2]\cdot 2H_2O$, $Cs_2[CH_2\{VO^V(\text{sal-nah})\}_2]\cdot 2H_2O$, $Cs_2[CH_2\{VO^V(\text{sal-inh})\}_2]\cdot 2H_2O$, $Cs_2[CH_2\{VO^V(\text{sal-bhz})\}_2]\cdot 2H_2O$ and $Cs_2[CH_2\{VO^V(\text{sal-fah})\}_2]\cdot 2H_2O$ exhibited around 89% conversion when using a substrate-to- H_2O_2 molar ratio of 1:2 with all three products^[29] as reported here. But the formation of 5-bromosalicylaldehyde is slightly lower, whereas that of 3,5-dibromosalicylaldehyde is higher than those found here.

Mechanism of Oxidative Bromination

The mode of action of V-dependent bromoperoxidase enzymes (V-BrPOs) has received much attention.^[1,5,6a,40b,47–51] The accepted mode of action of V-BrPOs involves the presence of vanadium in their active sites. This metal in the presence of hydrogen peroxide forms a peroxido vanadium derivative that oxidizes a bromide ion, thus forming a bromine equivalent intermediate. Such an intermediate may then either brominate an appropriate organic substrate or react with another molecule of Br^- to form bromine. The role of the V^V ion is to serve as a strong Lewis acid in the activation of the primary oxidant, H_2O_2 .

The suggestion that the high efficacy of this process is related to the formation of the intermediate, with the bromination reaction occurring in two different compartments of the enzymes – that is, the first step in a hydrophilic region of the protein and the second in a hydrophobic region – has led to model the reaction on the development of two-phase systems:^[5] (i) the vanadium precursor, H₂O₂ and KBr are dissolved in water, in which the formation of a peroxido V^V derivative and the oxidation of Br⁻ take place to form an intermediate; (ii) this intermediate is then transferred to the organic phase, a chlorinated solvent (i.e., CHCl₃ or CH₂Cl₂), in which the bromination of the substrate takes place. The processes that occur in the aqueous phase require acidic conditions, probably to promote the protonation of the peroxido moiety.

From the mechanistic point of view, there have been several attempts to elucidate the reaction pathways that involve the oxybromination reactions by combining reactivity analysis with, for example, spectroscopic techniques, mainly ⁵¹V NMR spectroscopy, and theoretical calculations.^[5,49–51] A mechanistic proposal^[5,6a,51] included two intermediates: a vanadium-bound hypobromite ion, which was responsible for the formation of the bromohydrin, and the second one, bromine, which was responsible for the formation of the dibromo products. Both pathways started from a hypobromite-like vanadium intermediate, formed in the reaction between the monoperoxido vanadium complex and Br⁻. However, direct evidence of the formation of either the hydroperoxido or the hypobromite-type vanadium intermediates has not yet been obtained, although the involvement of a V^V-containing brominating species has been confirmed in the two-phase reaction with adamantylideneadamantane, in which a salt that contains the bromiranium cation, together with the vanadate anion, was isolated and characterized.^[52]

The catalytic oxidation of styrene described in this study also follows the approach of using a two-phase system. In our systems we believe we have been able to identify the monoperoxido complexes **CV** and **CVI** (Scheme 3), which probably act as the oxidant of the Br⁻ ion as well as the oxidant of salicylaldehyde.

Thus, during oxidation, the vanadium in complexes **3–6** may coordinate with H₂O₂ to form V^V-oxidomonoperoxido species [e.g., **CV** (and **CVI**)] (Scheme 3). Under acidic conditions, oxidohydroxido complexes such as **CIV** might form, and in the presence of H₂O₂ **CVI** might also form. By adding KBr to these solutions, a new ⁵¹V NMR spectroscopic resonance appears at $\delta = -586$ ppm (Figure 12). We suggest that this resonance might correspond to species **CVII** (with a vanadium-bound hypobromite ion) or to a similar species that includes donor atoms of the ligand also bound to V^V. This species **CVII** might be responsible for the formation of the bromohydrin. Accordingly, the hypobromite-like species formed would be directly involved in the “Br⁺” transfer process or, at least, it is one of the active species in the bromination process.^[5,48]

The occurrence during the catalytic cycle of a species in which the equatorial peroxido oxygen is protonated and the

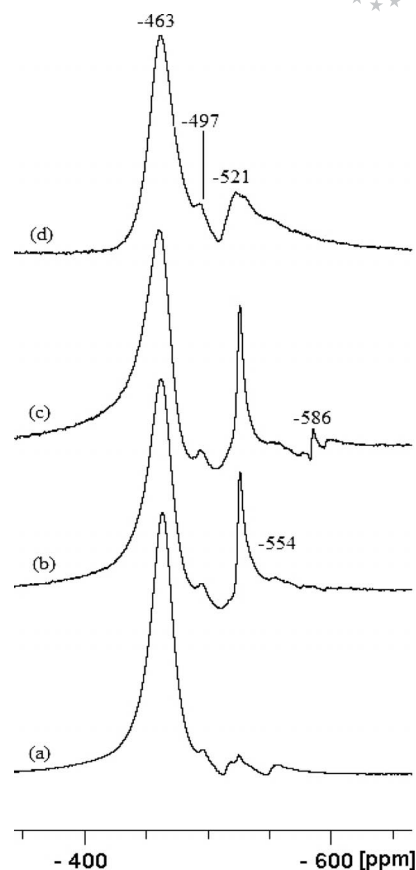


Figure 12. ⁵¹V NMR spectra for solutions (ca. 4 mM) of Cs₂[CH₂{VVO₂(sal-sbdt)}₂·2H₂O (**4**): (a) in DMSO, (b) with 4.0 equiv. of H₂O₂ (added as an aqueous solution of 30% H₂O₂) and (c) with 5 equiv. KBr (total) added to the solution of (b). (d) Solution of (c) after leaving the tube open for 24 h.

Br⁻ is prone to interact with the other peroxido oxygen has been proposed,^[49] with weak interactions between Br⁻ and V^V being also plausible prior to the oxo-transfer step.^[49] In the VHPO of the fungus *Curvularia inaequalis*, for example, a lysine side chain (from Lys353) also helps in the polarization of the V-bound peroxido moiety and tunes its reactivity.^[49] It is possible that in **CV** and/or **CVI** a similar type of effect may operate, but the data available does not allow us to discuss this further.

Antiamoebic Activity

The prepared VVO₂ complexes along with ligands **I** and **II** were screened for antiamoebic activity in vitro against the most common HMI:IMSS (from a human in Mexico, obtained from the Instituto Mexicano del Seguro Social), an axenic and highly virulent strain of *E. histolytica*. The IC₅₀ values are in the micromolar range and are shown in Table 7. The results were estimated by plotting a graph of logarithm of concentration versus percentage growth inhibition as compared with the untreated controls wells. The IC₅₀ values were obtained by interpolation in the corresponding dose response curves at 50% inhibition concentration. Among the sbdt series the ligand CH₂(sal-sbdt)₂

($IC_{50} = 0.56 \mu\text{M}$) and its V^V complexes $K_2[\text{CH}_2\{\text{V}^V\text{O}_2(\text{sal-sbdt})\}_2] \cdot 2\text{H}_2\text{O}$ (**3**) ($IC_{50} = 0.353 \mu\text{M}$) and $\text{Cs}_2[\text{CH}_2\{\text{V}^V\text{O}_2(\text{sal-sbdt})\}_2] \cdot 2\text{H}_2\text{O}$ (**4**) ($IC_{50} = 0.092 \mu\text{M}$) were found to be most active (IC_{50} lower than for metronidazole), whereas all the compounds of the smdt series were found to be much less active, except for $K_2[\text{CH}_2\{\text{V}^V\text{O}_2(\text{sal-smdt})\}_2] \cdot 2\text{H}_2\text{O}$ (**5**) ($IC_{50} = 0.85 \mu\text{M}$), which might be considered to be moderately active. Within the active sbdt series an increase in the activity was demonstrated with the incorporation of metal. The presence of a larger group (benzyl in sbdt) with higher hydrophobic character rather than the smaller group (methyl in smdt) is therefore important for the antiameobic activity in the present set of compounds tested. Among all the complexes it was also observed that $V^V\text{O}$ compounds are less active than $V^V\text{O}_2$ compounds. The reason why the V^V complexes are more active than the ligands is not clear. However, it is possible that complexation might favour permeation of the drugs through the lipid layer of the cell membrane.^[53] Whatever the actual species responsible for the biological effect measured, a significant increase in the antiameobic activity was previously found upon coordination of several related binucleating ligands to V^V .^[29] This clearly indicates that the vanadium

complexes might be potent inhibitors for the development of *E. histolytica* in vitro and that they are more active than the standard drug metronidazole.

Cytotoxicity of Compounds

The excellent antiameobic activity of ligand **I** and complexes **3**, **4** and **5** encouraged us to test their cytotoxicity. Therefore the cells were treated with various concentrations of ligand (**I**), compounds **3**, **4** and **5** or vehicle (DMSO) alone for 48 h (as indicated in Figure 13).

Cell survival was determined by an MTT assay. Cell viability was calculated as described in the Experimental Section as the mean from three independent experiments in which each treatment was done in triplicate. To assess the survival effects of the compounds, human breast cancer (MCF7) cells were used; 10000 cells per well in 200 μL of complete Dulbecco's modified Eagle's medium (DMEM) were plated. Different concentrations of the different compounds were added to the wells as indicated in Figure 13. An unusual trend in cytotoxicity was observed with the cell viability, especially for compounds **3**, **4** and **5**. Initially the viability increased with increasing compound concentration in the range 2.5–100 μM , then it decreased significantly. We do not know how to explain this behaviour but it may be related to the presence of foetal bovine serum in the medium. Its major component is bovine serum albumin and it is known that binding of metal complexes (e.g., vanadium compounds) to albumins may affect their activity; this would depend on the complex/albumin ratio.^[54]

The cell survival assay was also carried out in the presence of metronidazole and overall the IC_{50} value for all the compounds was found to be higher than 100 μM . Whatever the actual trend in cytotoxicity observed, these results show that all compounds evaluated are not particularly toxic, although they are more toxic than the standard drug metronidazole.

Table 7. Vanadium complexes **1–6** and their antiameobic activity against the HM1:IMSS strain of *E. histolytica*.

	IC_{50} [μM] ^[a]	s.d. ^[b]
I	0.56	0.01
1	7.18	0.01
3	0.353	0.01
4	0.092	0.01
II	5.4	0.005
2	6.31	0.01
5	0.85	0.01
6	8.55	0.02
Metronidazole	1.68	0.004

[a] The values were obtained from at least three separate assays done in duplicate. [b] Standard deviation.

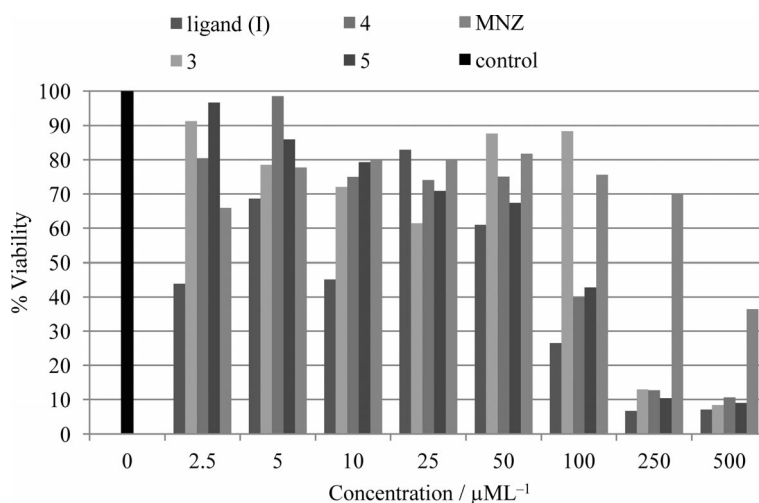


Figure 13. Percentage of viable cells after 48 h on human breast cancer (MCF7) cells upon incubation with various concentrations of ligand **I**, compounds **3**, **4**, **5**, and MNZ or vehicle control (DMSO). Cell survival was determined by the MTT [MTT=3-(4,5-dimethylthiazol-2-yl)-2,5-diphenyltetrazolium] bromide assay.

Among antiamebic studies reported earlier, the binuclear V^{VO}_2 complexes, $K_2[CH_2\{V^{VO}_2(sal-nah)\}_2] \cdot 2H_2O$, $Cs_2[CH_2\{V^{VO}_2(sal-inh)\}_2] \cdot 2H_2O$, $Cs_2[CH_2\{V^{VO}_2(sal-bhz)\}_2] \cdot 2H_2O$ and $Cs_2[CH_2\{V^{VO}_2(sal-fah)\}_2] \cdot 2H_2O$ are also active against the HM1:IMSS strains of *Entamoeba histolytica* ($IC_{50} = 0.32\text{--}0.54 \mu M$)^[29] but they are also relatively more toxic than the standard drug metronidazole.

Conclusion

The hydrazones $CH_2(H_2sal-sbdt)_2$ (**I**) and $CH_2(H_2sal-smtdt)_2$ (**II**) derived from 5,5'-methylenebis(salicylaldehyde) [$CH_2(Hsal)_2$] and *S*-benzylthiocarbamate $CH_2(Hsal-sbdt)_2$ (for **I**) or *S*-methylthiocarbamate $CH_2(Hsal-smtdt)_2$ (for **II**) and their V^{VO} and V^{VO}_2 complexes were synthesized and characterized. The complexes are dinuclear in the solid state and in solution, but no significant interactions were detected between the vanadium centres.

Solutions of the V^{VO} complexes [$CH_2\{V^{VO}(L)\}_2\} \cdot 2H_2O$ [$CH_2(HL)_2$ = **I** (**1**) and **II** (**2**)] were studied by UV/Vis, EPR and ^{51}V NMR spectroscopy, and also by adding H_2O_2 or acid (HCl). The speciation of solutions of the V^V complexes in MeOH and DMSO was also studied by the same spectroscopic techniques. The formation of several species was established, with some of them probably intermediates in the catalytic processes studied, namely, [$CH_2\{V^{VO}(O_2)(L)\}_2\}^{2-}$ and [$CH_2\{V^{VO}(OH)(L)\}_2\}$. Upon addition of acid (HCl), the V^V species present were partly reduced/hydrolyzed, thereby yielding several species, namely, the oxidohydroxido complex.

The V^{VO}_2 complexes **3–6** were shown to be functional models of vanadium-dependent haloperoxidases and satisfactorily catalyzed the oxidative bromination of salicylaldehyde and styrene. Complexes **4** and **6** are also catalyst precursors for the oxidation of styrene. Under optimized reaction conditions, the selectivity of the products formed by using $Cs_2[CH_2\{V^{VO}_2(sal-sbdt)\}_2] \cdot 2H_2O$ (**4**) as catalyst followed the order 1-phenylethane-1,2-diol > benzoic acid > phenylacetaldehyde > benzaldehyde > styrene oxide. In the case of $Cs_2[CH_2\{V^{VO}_2(sal-smtdt)\}_2] \cdot 2H_2O$ (**6**), however, the order was benzoic acid > 1-phenylethane-1,2-diol > benzaldehyde > styrene oxide > phenylacetaldehyde. Formation of styrene oxide in very poor yield suggested the conversion of styrene oxide into other products.

Plausible intermediates involved in these catalytic processes were established by UV/Vis, EPR and ^{51}V NMR spectroscopic studies, namely, monoperoxo- V^V complexes. A ^{51}V NMR spectroscopic peak detected at $\delta = -586$ ppm was probably due to a V^V complex that contained coordinated hypobromite ion. The vanadium complexes along with ligands **I** and **II** were also screened against HM1:IMSS strains of *Entamoeba histolytica*. The results showed that the IC_{50} values of compounds **3**, **4** and **5** are significantly lower than that of metronidazole, thereby suggesting that they might be promising drugs for the treatment of amoebiasis. Cytotoxicity studies show that the V^V complexes **3**, **4** and **5**, although very active against the

HM1:IMSS strains of *Entamoeba histolytica*, are not particularly toxic, although they are more toxic than the standard drug metronidazole.

Experimental Section

Materials: Acetylacetone (Hacac, E. Merck, India), styrene (Acros, USA), 30% aqueous H_2O_2 , KBr (E. Merck, India), salicylaldehyde, hydrazine hydrate, $CsOH \cdot H_2O$, benzyl chloride (S.D. fine chemicals, India), methyl iodide (Himedia, India) and 70% $HClO_4$ (Qualigens, India) were used as obtained. Other chemicals and solvents were of analytical reagent grade. *S*-Benzylthiocarbamate,^[55] *S*-methylthiocarbamate^[56] and 5,5'-methylbis(salicylaldehyde),^[57] $K[V^{VO}_2(sal-sbdt)(H_2O)]$ (**7**)^[28b] and $Na[V^{VO}_2(sal-smtdt)(H_2O)_2]$ (**8**)^[10g] were prepared as reported in the literature.

Instrumentation and Characterization Procedures: Elemental analyses of the compounds were carried out with an Elementar model Vario-El-III. IR spectra were recorded as KBr pellets with a Nicolet NEXUS Aligent 1100 series FTIR spectrometer. Electronic spectra were measured in methanol with a UV-1601 PC UV/Vis spectrophotometer. 1H NMR spectra were obtained with a Bruker 200, ^{13}C and ^{51}V NMR spectra with a Bruker Avance III 400 MHz spectrometer with the common parameter settings. NMR spectra were usually recorded in $[D_6]DMSO$, and δ (^{51}V) values are referenced relative to neat $V^{VO}Cl_3$ as external standard. Thermogravimetric analyses of the complexes were carried out under an oxygen atmosphere with a TG Stanton Redcroft STA 780 instrument. The magnetic susceptibilities were measured with a vibrating sample magnetometer model 155 supplied by Princeton Applied Research and by using nickel as standard. Diamagnetic corrections were carried out by using Pascal's constants.^[58] EPR spectra were recorded with a Bruker ESP 300E X-band spectrometer. The spin-Hamiltonian parameters were obtained by simulation of the spectra with the computer program by Rockenbauer and Korecz.^[38] A Thermo Nicolet gas chromatograph fitted with a HP-1 capillary column (30 m \times 0.25 mm \times 0.25 μm) and a flame ionization detector (FID) was used to analyze the reaction products and their quantifications were made on the basis of the relative peak area of the respective product. Oxidation and oxidative bromination of styrene have also been normalized from the set of calibration curve for styrene to get response factors, and the obtained results are nearly same within experimental error. The identity of the products was confirmed with a Clarus 500 GC-MS from Perkin-Elmer and by comparing the fragments of each product with the library available.

Preparation of $CH_2(H_2sal-sbdt)_2$ (I**) and $CH_2(H_2sal-smtdt)_2$ (**II**):** Compounds **I** and **II** were prepared by adapting methods reported in the literature.^[59] The preparation of representative ligand **I** is described here. A solution of 5,5'-methylbis(salicylaldehyde) (2.65 g, 10 mmol) was prepared in hot methanol (40 mL) and a solution of *S*-benzylthiocarbamate (3.966 g, 20 mmol) in methanol (20 mL) was added to the above. The reaction mixture was heated at reflux for 3 h on a water bath and was put in a refrigerator for 12 h. The deposited yellow solid was filtered, washed with methanol and dried in a desiccator. Finally, it was recrystallized from methanol to give a fine needle-like solid.

Data for $CH_2(H_2sal-sbdt)_2$ (I**):** Yield 6.45 g (67.7%). $C_{31}H_{28}N_4O_2S_4$ (616.83): calcd. C 60.36, H 4.58, N 9.08; found C 60.1, H 4.6, N 8.9.

Data for $CH_2(H_2sal-smtdt)_2$ (II**):** Yield 4.38 g (73.5%). $C_{19}H_{20}N_4O_2S_4$ (464.63): calcd. C 49.12, H 4.34, N 12.06; found C 49.2, H 4.4, N 12.1.

FULL PAPER

Preparation of $[\text{CH}_2\{\text{V}^{\text{VO}}(\text{sal-sbdt})(\text{H}_2\text{O})_2\}_2]$ (1): A filtered solution of $[\text{V}^{\text{VO}}(\text{acac})_2]$ (2.56 g, 10 mmol) in dry methanol (30 mL) was added to a filtered solution of **1** (3.08 g, 5 mmol) prepared in dry hot methanol (150 mL) while shaking the reaction flask. The reaction mixture was heated at reflux on a water bath for 4 h. After reducing the volume of the solvent to approximately 30 mL and keeping it at room temperature for 10 h, the separated brown solid was filtered, washed with methanol and dried in a desiccator with silica gel; yield 3.16 g (80.5%). μ_{eff} (293 K) = 1.73 μ_{B} . $\text{C}_{31}\text{H}_{28}\text{N}_4\text{O}_6\text{S}_4\text{V}_2$ (782.68): calcd. C 47.57, H 3.61, N 7.16; found C 47.7, H 3.5, N 7.2.

Preparation of $[\text{CH}_2\{\text{V}^{\text{VO}}(\text{sal-smdt})(\text{H}_2\text{O})_2\}_2]$ (2): Complex **2** was prepared from $[\text{V}^{\text{VO}}(\text{acac})_2]$ (0.530 g, 2 mmol) and **II** (0.464 g, 1 mmol) by the method outlined for **1**; yield 0.431 g (68.4%). μ_{eff} (293 K) = 1.71 μ_{B} . $\text{C}_{19}\text{H}_{20}\text{N}_4\text{O}_6\text{S}_4\text{V}_2$ (630.48): calcd. C 36.19, H 3.20, N 8.89; found C 36.4, H 3.0, N 8.9.

Preparation of $\text{K}_2[\text{CH}_2\{\text{V}^{\text{VO}}_2(\text{sal-sbdt})_2\}_2\cdot 2\text{H}_2\text{O}$ (3): Method A: A filtered solution of $[\text{V}^{\text{VO}}(\text{acac})_2]$ (0.530 g, 2 mmol) in methanol (15 mL) was added to a solution of **I** (0.616 g, 1 mmol) in methanol (450 mL) while stirring and was heated at reflux for 4 h. After adding KOH (0.224 g, 4.0 mmol) to the above, the reaction mixture was further heated at reflux for 2 h. The obtained light brown solution was allowed to oxidize aeri ally along with slow evaporation at room temperature. After 2 d the solution became yellow, its volume was reduced to approximately 10 mL and the solution was kept for 12 h at room temperature. A yellow solid of **3** separated out. This was filtered off, washed with methanol and dried in a desiccator with silica gel; yield 0.786 g (72.8%). $\text{C}_{31}\text{H}_{28}\text{K}_2\text{N}_4\text{O}_8\text{S}_4\text{V}_2$ (892.90): calcd. C 41.70, H 3.16, N 6.27; found C 41.8, H 3.1, N 6.3. ^{51}V NMR (400 MHz, $[\text{D}_6]\text{DMSO}$, 25 °C): $\delta = -462$ ppm. Method B: A mixture of $[\text{CH}_2\{\text{V}^{\text{VO}}(\text{sal-sbdt})(\text{H}_2\text{O})_2\}_2]$ (0.391 g, 0.5 mmol) and KOH (0.068 g, 1.2 mmol) in methanol (25 mL) was heated at reflux for 2 h and then left for aerial oxidation as well as slow evaporation of the solvent at room temperature. A yellow solid of **3** slowly precipitated out over approximately 3 d. This was filtered off, washed with cold methanol and dried in a desiccator with silica gel; yield 0.358 g (84.7%).

$\text{Cs}_2[\text{CH}_2\{\text{V}^{\text{VO}}_2(\text{sal-sbdt})_2\}_2\cdot 2\text{H}_2\text{O}$ (4): Method A: A filtered solution of $[\text{V}^{\text{VO}}(\text{acac})_2]$ (0.530 g, 2.0 mmol) in methanol (15 mL) was added to a solution of **I** (0.616 g, 1.0 mmol) in methanol (450 mL) while stirring and heated at reflux for 4 h. After adding $\text{CsOH}\cdot\text{H}_2\text{O}$ (0.403 g, 2.4 mmol), the reaction mixture was further heated at reflux for 2 h. The obtained light green solution was allowed to oxidize aeri ally while slowly evaporating at room temperature. After 2 d the green solution turned yellow, the volume was reduced to around 10 mL and the mixture was kept overnight at room temperature. A yellow solid of **4** separated out. This was filtered off, washed with methanol and dried in a desiccator with silica gel; yield 0.786 g (72.8%). $\text{C}_{31}\text{H}_{28}\text{Cs}_2\text{N}_4\text{O}_8\text{S}_4\text{V}_2$ (1080.49): calcd. C 34.46, H 2.61, N 5.19; found C 34.3, H 2.5, N 5.3. ^{51}V NMR (400 MHz, $[\text{D}_6]\text{DMSO}$, 25 °C): $\delta = -463$ ppm. Method B: A mixture of $[\text{CH}_2\{\text{V}^{\text{VO}}(\text{sal-sbdt})(\text{H}_2\text{O})_2\}_2]$ (**1**) (0.782 g, 1.0 mmol) and $\text{CsOH}\cdot\text{H}_2\text{O}$ (0.404 g, 2.4 mmol) in methanol (25 mL) was heated at reflux for 2 h and then left for aerial oxidation at room temperature over a period of approximately 3 d. A yellow solid of **4** precipitated out. This was filtered off, washed with methanol and dried in a desiccator with silica gel; yield 0.965 g (89.3%).

Preparation of $\text{K}_2[\text{CH}_2\{\text{V}^{\text{VO}}_2(\text{sal-smdt})_2\}_2\cdot 2\text{H}_2\text{O}$ (5): This complex was prepared by the procedures outlined for $\text{K}_2[\text{CH}_2\{\text{VO}_2(\text{sal-sbdt})_2\}_2\cdot 2\text{H}_2\text{O}$ (**3**) by using both methods A and B. Yield from method A: 0.513 g (73.9%); from method B: 0.602 g (86.7%). $\text{C}_{19}\text{H}_{20}\text{K}_2\text{N}_4\text{O}_8\text{S}_4\text{V}_2$ (740.71): calcd. C 30.81, H 2.72, N 7.56; found

C 30.9, H 2.7, N 7.5. ^{51}V NMR (400 MHz, $[\text{D}_6]\text{DMSO}$, 25 °C): $\delta = -462$ ppm.

Preparation of $\text{Cs}_2[\text{CH}_2\{\text{V}^{\text{VO}}_2(\text{sal-smdt})_2\}_2\cdot 2\text{H}_2\text{O}$ (6): This complex was prepared by the procedure outlined as method A and B for $\text{Cs}_2[\text{CH}_2\{\text{VO}_2(\text{sal-sbdt})_2\}_2\cdot 2\text{H}_2\text{O}$ (**4**). Yield from method A: 0.591 g (63.7%); from method B: 0.735 g (79.2%). $\text{C}_{19}\text{H}_{20}\text{Cs}_2\text{N}_4\text{O}_8\text{S}_4\text{V}_2$ (928.29): calcd. C 24.6, H 2.2, N 6.0; found C 24.5, H 2.1, N 6.2. ^{51}V NMR (400 MHz, $[\text{D}_6]\text{DMSO}$, 25 °C): $\delta = -463$ ppm.

Oxidation of Styrene: In a typical procedure, styrene (1.04 g, 10 mmol) and 30% (w/v) aqueous H_2O_2 (1.13 g, 10 mmol) were dissolved in methanol (7 mL) and the flask was maintained at 80 °C with an electrically heated oil bath. The catalyst to be tested, either $\text{Cs}_2[\text{CH}_2\{\text{V}^{\text{VO}}_2(\text{sal-smdt})_2\}_2\cdot 2\text{H}_2\text{O}$ (**6**) (0.0010 g, 0.0012 mmol) or $\text{Cs}_2[\text{CH}_2\{\text{V}^{\text{VO}}_2(\text{sal-sbdt})_2\}_2\cdot 2\text{H}_2\text{O}$ (**4**) (0.0030 g, 0.0028 mmol), was added and the reaction mixture was stirred for 8 h. The products were extracted in *n*-heptane and analyzed quantitatively by GC with a Thermo trace gas chromatograph that had an HP-1 column (30 m \times 0.25 mm \times 0.25 μm) and an FID detector. The products were identified by GC-MS with a Perkin-Elmer Clarus 500 equipped with an Elite-5 column (30 m \times 0.25 mm \times 0.25 μm). Complexes **7** and **8** were also studied under similar conditions.

Oxidative Bromination of Salicylaldehyde: Complexes **3-8** were used as catalyst precursors to carry out oxidative brominations. In a typical reaction, salicylaldehyde (2.44 g, 20 mmol) was added to an aqueous solution (40 mL) of KBr (5.95 g, 50 mmol), followed by addition of aqueous 30% H_2O_2 (15 g, 120 mmol) in a 100 mL reaction flask. The catalyst (e.g., 0.0070 g) and 70% HClO_4 (4.02 g, 20 mmol) were added and the reaction mixture was stirred at room temperature. Three additional 20 mmol portions of 70% HClO_4 were further added to the reaction mixture at $t = 30, 60$ and 90 min of reaction, in three equal portions, under continuous stirring. In all batches, the experimental conditions (e.g., stirring speed, the size of the magnetic bar and reaction flask) were kept as similar as possible. After 7 h, the white solid product that had separated was filtered off, washed with water and dried. The crude mass was dissolved in CH_2Cl_2 ; insoluble material, if any, was removed by filtration, and the solvent evaporated. A CH_2Cl_2 solution of this material was subjected to gas chromatography, and the identity of the products was confirmed by GC-MS.

Oxidative Bromination of Styrene: Complexes **3-8** were also used as catalyst precursors to carry out the oxidative bromination of styrene. In a typical reaction, styrene (1.04 g, 10 mmol) was added to an aqueous solution (20 mL) of KBr (3.57 g, 30 mmol), followed by the addition of CH_2Cl_2 (20 mL) and 30% aqueous H_2O_2 (3.40 g, 30 mmol) in a 100 mL reaction flask. The catalyst (0.0010 g) and 70% HClO_4 (1.43 g, 10 mmol) were added, and the reaction mixture was stirred at room temperature. Three additional 10 mmol portions of 70% HClO_4 were further added after every 10 min with continuous stirring. In all batches, the experimental conditions (e.g., stirring speed, the size of the magnetic bar and reaction flask) were kept as similar as possible. After 1 h, the orange organic layer was separated with a separatory funnel, washed with water and dried. The crude mass was redissolved in CH_2Cl_2 ; insoluble material, if any, was removed by filtration, and the solvent evaporated. The reaction products were separated by using a silica gel column. Elution of the column with 1% CH_2Cl_2 in *n*-hexane first separated a mixture of bromo derivatives followed by 1-phenylethane-1,2-diol. The two bromo derivatives were finally separated from each other with the silica gel column again by eluting with pure *n*-hexane. The identity of all products was confirmed by GC-MS and ^1H NMR spectroscopy.

1,2-Dibromo-1-phenylethane: ^1H NMR (CDCl_3): $\delta = 7.29\text{--}7.39$ (m, 5 H, aromatic), 5.11–5.13 (q, 1 H, CH), 3.97–4.06 (septet, 2 H, CH_2) ppm.

1-Phenylethane-1,2-diol: ^1H NMR (CDCl_3): $\delta = 7.29\text{--}7.39$ (m, 5 H, aromatic), 4.9 (q, 1 H, CH), 3.5 (q, 1 H of CH_2), 3.6 (q, 1 H of CH_2), 2.7 (br., 1 H, OH) ppm.

2-Bromo-1-phenylethane-1-ol: ^1H NMR (CDCl_3): $\delta = 7.29\text{--}7.39$ (m, 5 H, aromatic), 5.1 (q, 1 H, CH), 3.9 (septate, 2 H, CH_2) ppm.

In Vitro Testing Against *E. histolytica*: Ligands **I** and **II** and their complexes **1** to **6** were screened in vitro for antiamoebic activity against the HM1:IMSS strain of *E. histolytica* by using a microplate method. *E. histolytica* trophozoites were cultured in TYIS-33 growth medium. DMSO (40 μL) was added to all samples (1 mg) followed by enough fresh culture medium to obtain a concentration of 1 mg mL^{-1} . The maximum concentration of DMSO in the tests did not exceed 0.1%, at which level no inhibition of amoebal growth occurred. Samples were dissolved or suspended by mild sonication for a few minutes to obtain a clear solution, then further dilution with medium to obtain a concentration of 0.1 mg mL^{-1} . Twofold serial dilutions were made in the wells of a 96-well microtitre plate (costar) in the medium (170 μL). Each test included metronidazole as the standard amoebicidal drug; control wells (culture medium plus amoebae) were prepared from a confluent culture by pouring off the medium, adding medium (2 mL) and chilling the culture on ice for 8 min to detach the organisms from the side of the flask. The number of the amoeba per millilitre was estimated with a haemocytometer, and trypan blue exclusion was used to confirm viability. The cell suspension used was diluted to 10^5 organism per millilitre by adding fresh medium, and 170 μL of this suspension was added to the test and control well in the plate with multi-channel pipette so that the wells were completely filled (total volume, 340 μL). An inoculum of 1.7×10^4 organisms per well was chosen so that confluent, but not excessive, growth took place in the control wells. The plate was sealed with expanded polystyrene (0.5 mm), secured with tape, placed in a modular incubating chamber (flow laboratories, High Wycombe, UK) and gassed for 10 min with nitrogen before incubation at 37 $^\circ\text{C}$ for 72 h.

Assessment of Antiamoebic Activity: After incubation, the growth of amoebae in the plate was checked with a low-power microscope. The culture medium was removed by inverting the plate and shaking gently. The plate was then immediately washed once in 0.9% NaCl at 37 $^\circ\text{C}$. This procedure was completed quickly, and the plate was not allowed to cool so as to prevent the detachment of amoebae. The plate was allowed to dry at room temperature and the amoebae were fixed with chilled (-20 $^\circ\text{C}$) methanol for 15 min, and when dry, stained with 0.5% aqueous eosin for 15 min. The stained plate was washed once with tap water and then twice with distilled water and allowed to dry. A 200 μL portion of 0.1 N NaOH solutions was added to each well to dissolve the protein and release the dye. The optical density of the resulting solution in each well was determined at 490 nm with a microplate reader. The percentage of inhibition of amoebal growth was calculated from the optical densities of the control and test wells and plotted against the logarithm of the dose of the drug tested. Linear regression analysis was used to determine the best-fit straight line from which the IC_{50} value was found.

Cytotoxicity Evaluation: The human breast cancer (MCF7) cells were obtained from NCCS (Pune, India). The cells were cultured in DMEM (Sigma) with 10% foetal bovine serum and 1% penicillin/streptomycin/neomycin. The effect of active ligand **I**, compounds **3**, **4**, **5**, and the standard drug (metronidazole) on cell proliferation was measured by using an MTT-based assay.^[60] Briefly, the cells

(10000 per well) were incubated in triplicate in a 96-well plate in the presence of various concentrations of ligand **I**, compounds **3**, **4** and **5** as well as metronidazole or vehicle (DMSO) alone in a final volume of 200 μL at 37 $^\circ\text{C}$ in a humidified chamber for 48 h. At the end of this time period, MTT solution (20 μL) [5 mg per mL in phosphate buffer solution (PBS)] was added to each well, and the cells were incubated at 37 $^\circ\text{C}$ in a humidified chamber for 4 h. After 4 h, the supernatant was removed from each well. The coloured formazan crystals produced from MTT were dissolved in DMSO (200 μL), and then the absorbance (A) value was measured at 570 nm with a multiscanner autoreader. The following formula was used for the calculation of the percentage of cell viability (CV): $\text{CV} [\%] = (A \text{ of the experimental samples} / A \text{ of the control}) \times 100$.

Supporting Information (see footnote on the first page of this article): Electronic and ^{13}C NMR spectral data, IR and ^1H NMR spectra of representative ligands and complexes, speciation studies by electronic, ^{51}V NMR and EPR spectroscopy and catalytic data on the oxidative bromination of styrene.

Acknowledgments

M. R. M. thanks the Department of Science and Technology (DST), Government of India, New Delhi (SR/S1/IC-32/2010) for financial support of the work. C. H. and A. A. K. acknowledge the Council of Scientific and Industrial Research (CSIR), New Delhi for a fellowship. J. C. P. and A. K. thank the Fundação para a Ciência e Tecnologia (FEDER), project PEst-OE/QUI/UI0100/2011, and the Portuguese NMR Network (IST-UTL Center), grant number SFRH/BPD/34835/2007 for support.

- [1] D. Rehder, *Bioinorganic Vanadium Chemistry*, Wiley, New York, 2008.
- [2] a) A. Butler, C. J. Carrano, *Coord. Chem. Rev.* **1991**, *109*, 61–105; b) A. Butler, M. J. Clague, G. E. Meister, *Chem. Rev.* **1994**, *94*, 625–638.
- [3] D. Gambino, *Coord. Chem. Rev.* **2011**, *255*, 2193–2203.
- [4] M. R. Maurya, *Coord. Chem. Rev.* **2003**, *237*, 163–181.
- [5] V. Conte, B. Floris, *Inorg. Chim. Acta* **2010**, *363*, 1935–1946.
- [6] a) V. Conte, A. Coletti, B. Floris, G. Licini, C. Zonta, *Coord. Chem. Rev.* **2011**, *255*, 2165–2177; b) J. A. L. da Silva, J. J. R. Fraústo da Silva, A. J. L. Pombeiro, *Coord. Chem. Rev.* **2011**, *255*, 2232–2248; c) M. R. Maurya, A. Kumar, J. Costa Pessoa, *Coord. Chem. Rev.* **2011**, *255*, 2315–2344; d) M. R. Maurya, J. Costa Pessoa, *J. Organomet. Chem.* **2011**, *696*, 244–254.
- [7] M. R. Maurya, *J. Chem. Sci.* **2011**, *123*, 215–228.
- [8] I. Correia, S. Aksu, P. Adão, J. Costa Pessoa, R. A. Sheldon, I. W. C. E. Arends, *J. Inorg. Biochem.* **2008**, *102*, 318–329.
- [9] a) A. Messerschmidt, R. Wever, *Proc. Natl. Acad. Sci. USA* **1996**, *93*, 392–396; b) M. Weyand, H. J. Hecht, M. Kiesz, M. F. Liaud, H. Vilter, D. Schomburg, *J. Mol. Biol.* **1999**, *293*, 595–611; c) M. I. Isupov, A. R. Dalby, A. Brindley, Y. Izumi, T. Tanabe, G. N. Murshudov, J. A. Littlechild, *J. Mol. Biol.* **2000**, *299*, 1035–1049.
- [10] a) C. R. Cornman, J. Kampf, M. S. Lah, V. L. Pecoraro, *Inorg. Chem.* **1992**, *31*, 2035–2043; b) C. R. Cornman, G. J. Colpas, J. D. Hoeschele, J. Kampf, V. L. Pecoraro, *J. Am. Chem. Soc.* **1992**, *114*, 9925–9933; c) C. R. Cornman, J. Kampf, V. L. Pecoraro, *Inorg. Chem.* **1992**, *31*, 1981–1983; d) V. Vergopoulos, W. Priebsch, M. Fritzsche, D. Rehder, *Inorg. Chem.* **1993**, *32*, 1844–1849; e) L. J. Calviou, J. M. Arber, D. Collison, C. D. Garner, W. Clegg, *J. Chem. Soc., Chem. Commun.* **1992**, 654–656; f) A. D. Keramidis, S. M. Miller, O. P. Anderson, D. C. Crans, *J. Am. Chem. Soc.* **1997**, *119*, 8901–8915; g) S. Samanta, S. K. Dutta, M. Chaudhury, *J. Chem. Soc.* **2006**, *118*, 475–486; h) S. K. Dutta, S. Samanta, S. Mukhopadhyay, P. Burckel, A. A. Pinkerton, M. Chaudhury, *Inorg. Chem.* **2002**, *41*, 2946–

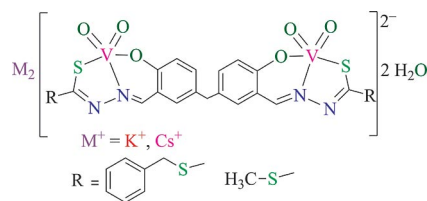
FULL PAPER

- 2952; i) S. Samanta, D. Ghosh, S. Mukhopadhyay, A. Endo, T. J. R. Weakley, M. Chaudhury, *Inorg. Chem.* **2003**, *42*, 1508–1517; j) M. R. Maurya, A. Kumar, M. Ebel, D. Rehder, *Inorg. Chem.* **2006**, *45*, 5924–5937.
- [11] S. Rayati, N. Sadeghzadeh, H. R. Khavasi, *Inorg. Chem. Commun.* **2007**, *10*, 1545–1548.
- [12] S. Rayati, N. Torabi, M. Koliaei, F. Ashouri, S. Mohebbi, A. Wojtczak, A. Kozakiewicz, *Appl. Catal. A: Gen.* **2008**, *346*, 65–71.
- [13] S. Rayati, N. Torabi, A. Ghaemi, S. Mohebbi, A. Wojtczak, A. Kozakiewicz, *Inorg. Chim. Acta* **2008**, *361*, 1239–1248.
- [14] S. Mohebbi, D. M. Boghaei, A. H. Sarvestani, A. Salimi, *Appl. Catal. A: Gen.* **2005**, *278*, 263–267.
- [15] M. R. Maurya, A. K. Chandrakar, S. Chand, *J. Mol. Catal. A* **2007**, *270*, 225–235.
- [16] a) M. R. Maurya, U. Kumar, I. Correia, P. Adão, J. Costa Pessoa, *Eur. J. Inorg. Chem.* **2008**, 577–587; b) M. R. Maurya, A. Arya, U. Kumar, A. Kumar, F. Avecilla, J. Costa Pessoa, *Dalton Trans.* **2009**, 9555–9566.
- [17] M. R. Maurya, S. Sikarwar, P. Manikandan, *Appl. Catal. A: Gen.* **2006**, *315*, 74–82.
- [18] M. R. Maurya, A. Kumar, P. Manikandan, S. Chand, *Appl. Catal. A: Gen.* **2004**, *277*, 45–53.
- [19] P. Noblíá, E. J. Baran, L. Otero, P. Draper, H. Cerecetto, M. González, O. E. Piro, E. E. Castellano, T. Inohara, Y. Adachi, H. Sakurai, D. Gambino, *Eur. J. Inorg. Chem.* **2004**, 322–328.
- [20] D. I. Edwards, *J. Antimicrob. Chemother.* **1993**, *31*, 201–210.
- [21] M. M. L. Nigro, A. B. Gadano, M. A. Carballo, *Toxicol. in vitro* **2001**, *15*, 209–213.
- [22] S. N. J. Moreno, R. Docampo, *Environ. Health Perspect.* **1985**, *64*, 199–208.
- [23] Y. Akgun, I. H. Tacyldz, Y. Celik, *World J. Surg.* **1999**, *23*, 102–106.
- [24] T. H. Conner, M. Stoeckel, J. Evrard, M. S. Legator, *Cancer Res.* **1977**, *37*, 629–633.
- [25] K. Kapoor, M. Chandra, D. Nag, J. K. Paliwal, R. C. Gupta, R. C. Saxena, *Int. J. Clin. Pharmacol. Res.* **1999**, *19*, 83–88.
- [26] H. S. Rosenkranz, W. T. Speck, *Biochem. Biophys. Res. Commun.* **1975**, *66*, 520–525.
- [27] D. A. Rowley, R. C. Knight, I. M. Skolimowski, D. I. Edwards, *Biochem. Pharmacol.* **1980**, *29*, 2095–2098.
- [28] a) N. Bharati, Shailendra, M. T. G. Garza, D. E. Cruz-Vega, J. Castro-Garza, K. Saleem, F. Naqvi, M. R. Maurya, A. Azam, *Bioorg. Med. Chem. Lett.* **2002**, *12*, 869–871; b) M. R. Maurya, S. Khurana, Shailendra, A. Azam, W. Zhang, D. Rehder, *Eur. J. Inorg. Chem.* **2003**, 1966–1973; c) M. R. Maurya, S. Agarwal, M. Abid, A. Azam, C. Bader, M. Ebel, D. Rehder, *Dalton Trans.* **2006**, 937–947; d) M. R. Maurya, A. Kumar, A. R. Bhat, A. Azam, C. Bader, D. Rehder, *Inorg. Chem.* **2006**, *45*, 1260–1269; e) M. R. Maurya, A. Kumar, M. Abid, A. Azam, *Inorg. Chim. Acta* **2006**, *359*, 2439–2447.
- [29] a) M. R. Maurya, A. A. Khan, A. Azam, S. Ranjan, N. Mondal, A. Kumar, J. Costa Pessoa, *Eur. J. Inorg. Chem.* **2009**, 5377–5390; b) M. R. Maurya, A. A. Khan, A. Azam, S. Ranjan, N. Mondal, A. Kumar, F. Avecillam, J. Costa Pessoa, *Dalton Trans.* **2010**, *39*, 1345–1360.
- [30] S. P. Perlepes, D. Nicholls, M. R. Harison, *Inorg. Chim. Acta* **1985**, *102*, 137–143.
- [31] M. R. Maurya, S. Agarwal, C. Bader, D. Rehder, *Eur. J. Inorg. Chem.* **2005**, 147–157.
- [32] M. R. Maurya, S. Khurana, W. Zhang, D. Rehder, *Eur. J. Inorg. Chem.* **2002**, 1749–1760.
- [33] D. Rehder, C. Weidemann, A. Duch, W. Priebisch, *Inorg. Chem.* **1988**, *27*, 584–587.
- [34] K. Wüthrich, *Helv. Chim. Acta* **1965**, *48*, 1012–1017.
- [35] N. D. Chasteen, in: *Biological Magnetic Resonance* (Ed.: J. Reuben), Plenum, New York, **1981**, p. 53.
- [36] A. J. Tasiopoulos, A. N. Troganis, A. Evangelou, C. P. Raptopoulou, A. Terzis, Y. Deligiannakis, T. A. Kabanos, *Chem. Eur. J.* **1999**, *5*, 910–921.
- [37] a) I. Cavaco, J. Costa Pessoa, M. T. Duarte, R. T. Henriques, P. M. Matias, R. D. Gillard, *J. Chem. Soc., Dalton Trans.* **1996**, 1989–1996; b) J. Costa Pessoa, I. Cavaco, I. Correia, D. Costa, R. T. Henriques, R. D. Gillard, *Inorg. Chim. Acta* **2000**, *305*, 7–13.
- [38] For computer simulations of EPR spectra, see: A. Rockenbauer, L. Korecz, *Appl. Magn. Reson.* **1996**, *10*, 29–43.
- [39] a) M. R. Maurya, A. Kumar, *J. Mol. Catal. A* **2006**, *250*, 190–198; b) D. Rehder, G. Santoni, G. M. Licini, C. Schulzke, B. Meier, *Coord. Chem. Rev.* **2003**, *237*, 53–63; c) M. R. Maurya, M. Kumar, A. Kumar, J. Costa Pessoa, *Dalton Trans.* **2008**, 4220–4232; d) M. R. Maurya, U. Kumar, P. Manikandan, *Eur. J. Inorg. Chem.* **2007**, 2303–2314.
- [40] a) G. J. Colpas, B. J. Hamstra, J. W. Kampf, V. L. Pecoraro, *J. Am. Chem. Soc.* **1996**, *118*, 3469–3478; b) B. J. Hamstra, G. J. Colpas, V. L. Pecoraro, *Inorg. Chem.* **1998**, *37*, 949–955.
- [41] I. Cavaco, J. Costa Pessoa, S. Luz, M. T. L. Duarte, P. M. Matias, R. T. Henriques, R. D. Gillard, *Polyhedron* **1995**, *14*, 429–439.
- [42] a) M. R. Maurya, A. K. Chandrakar, S. Chand, *J. Mol. Catal. A* **2007**, *263*, 227–237; b) M. R. Maurya, U. Kumar, I. Correia, P. Adão, J. Costa Pessoa, *Eur. J. Inorg. Chem.* **2008**, 577–587.
- [43] W. Plass, A. Pohlmann, H.-P. Yozgatli, *J. Inorg. Biochem.* **2000**, *80*, 181–183.
- [44] K. Fukui, H. Ohya-Nishiguchi, H. Kamada, *Inorg. Chem.* **1998**, *37*, 2326–2327.
- [45] a) P. Adão, J. Costa Pessoa, R. T. Henriques, M. L. Kuznetsov, F. Avecilla, M. R. Maurya, U. Kumar, I. Correia, *Inorg. Chem.* **2009**, *48*, 3542–3561; b) M. R. Maurya, A. K. Chandrakar, S. Chand, *J. Mol. Catal. A* **2007**, *274*, 192–201; c) M. R. Maurya, A. K. Chandrakar, S. Chand, *J. Mol. Catal. A* **2007**, *263*, 227–237.
- [46] M. R. Maurya, M. Kumar, A. Arya, *Catal. Commun.* **2008**, *10*, 187–191.
- [47] D. C. Crans, J. J. Smees, E. Gaidamauskas, L. Yang, *Chem. Rev.* **2004**, *104*, 849–902.
- [48] M. J. Clague, N. L. Keder, A. Butler, *Inorg. Chem.* **1993**, *32*, 4754–4761.
- [49] G. Zampella, P. Fantucci, V. L. Pecoraro, L. De Gioia, *J. Am. Chem. Soc.* **2005**, *127*, 953–960.
- [50] O. Bortolini, M. Carraro, V. Conte, S. Moro, *J. Inorg. Biochem.* **2000**, *80*, 41–49.
- [51] J. Littlechild, E. Garcia-Rodriguez, E. Coupe, A. Watts, M. Isupov, in: *Vanadium: The Versatile Metal* (Eds.: K. Kustin, J. Costa Pessoa, D. C. Crans), ACS Series Book, **2007**, *974*, pp. 136–147.
- [52] O. Bortolini, C. Chiappe, V. Conte, M. Carraro, *Eur. J. Org. Chem.* **1999**, 3237–3239.
- [53] A. M. Ramadan, *J. Inorg. Biochem.* **1997**, *65*, 183–189.
- [54] J. Costa Pessoa, I. Tomaz, *Curr. Med. Chem.* **2010**, *17*, 3701–3738.
- [55] M. A. Ali, M. T. H. Tarafder, *J. Inorg. Nucl. Chem.* **1977**, *39*, 1785–1791.
- [56] M. Das, S. E. Livingstone, *Inorg. Chim. Acta* **1976**, *19*, 5–10.
- [57] C. S. Marvel, N. Tarkoy, *J. Am. Chem. Soc.* **1957**, *79*, 6000–6002.
- [58] R. L. Dutta, A. Syamal, *Elements of Magnetochemistry*, 2nd ed., Affiliated East-West Press, New Delhi, **1993**, p. 8.
- [59] M. R. Maurya, D. C. Antony, S. Gopinathan, C. Gopinathan, *Bull. Chem. Soc. Jpn.* **1995**, *68*, 554–565.
- [60] T. Mosmann, *J. Immunol. Methods* **1983**, *65*, 55–63.

Received: January 6, 2012

Published Online: ■

Cationic binuclear dioxovanadium(V) complexes have been isolated and their characterization, catalytic and antiamoebic properties are reported



**M. R. Maurya,* C. Haldar, A. A. Khan,
A. Azam, A. Salahuddin, A. Kumar,
J. Costa Pessoa*** 1–19

Synthesis, Characterization, Catalytic and Antiamoebic Activity of Vanadium Complexes of Binucleating Bis(dibasic tridentate ONS donor) Ligand Systems 

Keywords: Vanadium / Enzyme models / Antiprotozoal agents / Hydrazones / EPR spectroscopy / NMR spectroscopy